UNIVERSIDADE FEDERAL RURAL DE PERNAMBUCO
UNIDADE ACADÊMICA DE SERRA TALHADA
LICENCIATURA EM QUÍMICA

O PAPEL DOS COMPOSTOS AUXINO-SIMILARES EXTRAÍDOS DE HIDROCARVÕES DE RESÍDUOS DE MILHO NA GERMINAÇÃO DE SEMENTES-TESTE DE *Lactuca sativa*

Edson Thiago Gomes de Lima

Serra Talhada, PE
Dezembro de 2022

EDSON THIAGO GOMES DE LIMA

O PAPEL DOS COMPOSTOS AUXINO-SIMILARES EXTRAÍDOS DE HIDROCARVÕES DE RESÍDUOS DE MILHO NA GERMINAÇÃO DE SEMENTES-TESTE DE *Lactuca sativa*

Trabalho de Conclusão de Curso (TCC) apresentado à Coordenação do Curso de Licenciatura em Química, na modalidade Artigo Científico, como pré-requisito para a obtenção do título de Licenciado em Química, pela Universidade Federal Rural de Pernambuco.

Orientador: Prof. Dr. Ramom Rachide Nunes

Serra Talhada, PE
Dezembro de 2022

RESUMO

Neste trabalho estudou-se a atividade auxino-similar de hidrocarvões líquidos e sólidos obtido a partir de resíduos de milho, preparados por carbonização hidrotérmica (HTC). Os bioensaios foram realizados testando concentrações do hidrocarvão líquido na faixa de 0,0557-5570,0 mg de carbono L^{-1}; e hidrocarvão sólido na faixa de 0,026-2600,0 mg de carbono L^{-1}. A matéria orgânica dissolvida (DOM) foi extraída para realização de testes utilizando hidrocarvão sólido. Os bioensaios foram realizados com sementes de *Lactuca sativa*. Os métodos instrumentais MEV, ATR-FTIR e Py-GC/MS foram usados para avaliar o efeito da HTC na produção/composição de hidrocarvão. O hidrocarvão líquido apresentou intensa bioatividade, inibindo completamente a germinação das sementes-teste em concentrações acima de 696 mg C L^{-1}. O hidrocarvão líquido foi consideravelmente mais bioativo que a DOM, mesmo apresentando efeito auxino-similar nos testes de germinação. A análise MEV mostrou como a HTC transformou a superfície da matéria-prima, abrindo poros e sulcos nos hidrocarvões. O ATR-FTIR também mostrou que a HTC mudou a composição química dos resíduos de milho, reduzindo os grupos hidroxila e enriquecendo o material com grupos funcionais aromáticos. O Py-GC/MS permitiu a identificação das moléculas envolvidas nos efeitos do tipo AIA: ácidos carboxílicos (lineares e aromáticos) e aminoácidos. A concentração de mais moléculas bioativas, ao invés de sua simples presença na fração do hidrocarvão, determinou o efeito bioestimulante, além de uma boa regressão linear entre a atividade auxino-similar e a concentração de moléculas ativas estimulantes.

Palavras-chave: Carbonização hidrotérmica, Compostos orgânicos, Atividade hormono-similar, Propriedade auxino-similar, Matéria orgânica dissolvida.

ABSTRACT

This work studied the auxin-like activity of liquid and solid hydrochar obtained from corn overground biomass, prepared using hydrothermal carbonization (HTC). Bioassays were performed by testing liquid hydrochar concentrations in the range of 0.0557-5570.0 mg carbon L^{-1}; and solid hydrochar in the range 0.026-2600.0 mg carbon L^{-1}. Dissolved organic matter (DOM) was extracted to perform tests using solid hydrochar. Bioassays were performed using seeds of *Lactuca sativa*. SEM, ATR-FTIR, and Py-GC/MS instrumental methods were used to assess the effect of HTC on hydrochar production/composition. Liquid hydrochar presented an intense bioactivity, completely inhibiting the germination of testing seeds at concentrations above 696 mg C L^{-1}. Liquid hydrochar also was considerably more bioactive than the DOM, even it has shown auxin-like effect in the germination tests. SEM analysis showed how HTC transformed the feedstock surface, by opening pores and grooves in the hydrochars. ATR-FTIR also showed how the HTC changed the chemical composition of corn waste, reducing hydroxyl groups and enriching the material by aromatic functional groups. Py-GC/MS allowed the identification of the molecules involved in IAA-like effects: carboxylic acids (linear and aromatic) and amino acids. The concentration of more bio-active molecules, rather than their simple presence in the hydrochar fraction, determined the bio-stimulating effect, besides a good linear regression between auxin-like activity and the concentration of active stimulating molecules.

Keywords: Hydrothermal carbonization, Organic compounds, Hormone-like activity, Auxin-like property, Dissolved organic matter.

1. INTRODUÇÃO

O milho (*Zea mays*) é uma das culturas mais importantes do mundo, com produção global de 1,168 bilhão de toneladas na safra de 2022/2023 (USDA, 2022). Entretanto, além da alta produção também é gerada uma elevada quantidade de resíduos agrícolas, que podem ser prejudiciais ao meio ambiente quando descartados de forma inadequada. Para evitar a poluição, tratamentos químicos, físicos e biológicos específicos têm sido adotados para reduzir a quantidade de resíduos, potencializando os sistemas de aproveitamento/reciclagem de resíduos de milho (AWOGBEMI; KALLON, 2022).

Nesta perspectiva, a carbonização hidrotérmica (HTC) é relatada como um tratamento eficaz para os resíduos agrícolas, agregando valor ao melhorar a qualidade da matéria orgânica (MO) e a disponibilidade de nutrientes. Em geral, o HTC é realizado usando água como meio reacional, temperaturas moderadas (180-250ºC) e pressão autogerada. Como produto, a HTC converte a matéria-prima úmida em um material carbonáceo, denominado hidrocarvão. Além disso, a HTC também gera uma fração líquida derivada da fusão/dissolução das moléculas orgânicas mais lábeis em solução. A HTC também é considerada um método econômico e ecológico, devido à baixa energia aplicada e a pequena geração de subprodutos indesejados, como CO_2 (AYODELE et al., 2022; CHEN et al., 2021; LANG et al., 2022). Em geral, durante a HTC, a água em estado subcrítico promove transformações na matéria-prima. Primeiramente, o MO sofre hidrólise, acompanhada pela desidratação e descarboxilação. Além disso, as cadeias carbônicas são condensadas e aromatizadas, proporcionando um material com maior teor de carbono elementar quando comparado à matéria-prima (HARIS et al., 2022; LIN et al., 2022; MARIUZZA et al., 2022).

Por fim, o hidrocarvão apresenta baixas razões atômicas O/C e H/C, indicando uma estabilidade do MO. Além disso, o hidrocarvão também apresenta alta concentração de grupos funcionais e alta área superficial, que influenciam positivamente na capacidade de troca catiônica (CTC), além da retenção e disponibilidade de nutrientes (BENTO et al., 2021; KHOSRAVI et al., 2022; MOHAMMADI et al., 2022; ZHANG; QIN; YI, 2021).

Dependendo das características do hidrocarvão, diferentes formas de uso podem ser destinadas, por exemplo, como insumo agrícola (HOU et al., 2020; KAVINDI et al., 2022), material adsorvente (IGHALO et al., 2022; LANG et al., 2021), combustível sólido (KANG et al., 2019; MARIUZZA et al., 2022), como catalisador (QUEVEDO-AMADOR et al., 2022; SHUANG et al., 2022), etc. A utilização agrícola do hidrocarvão é bastante comum, sendo aplicado principalmente na remediação ambiental, como condicionador de solo e em sistemas modernos de agricultura, fornecendo MO e nutrientes ao solo, visando promover a nutrição e a produção vegetal (BENTO et al., 2021; KHOSRAVI et al., 2022).

Muitos estudos têm relatado o uso potencial de hidrocarvões na agricultura. Bento et al. (2019) avaliaram a liberação de nutrientes e MO do hidrocarvão de vinhaça em diferentes solos,

concluindo que o hidrocarvão foi um fertilizante orgânico eficiente, com potencial para melhorar a produtividade agrícola. Hou et al. (2020) mostraram como a aplicação de hidrocarvão de serragem em uma cultura de arroz aumentou a produtividade e reduziu significativamente a emissão de gases de efeito estufa. Kavindi et al. (2022) produziram hidrocarvões a partir de palha de arroz e lodo de esgoto, mostrando sua eficiência na remediação de solos contaminados por Cr(VI).

Diversos estudos têm indicado que parte do papel da MO na promoção do desenvolvimento vegetal está associada à presença de hormônios vegetais, principalmente os do grupo das auxinas. Por outro lado, alguns autores relataram a presença de moléculas orgânicas diferentes da auxina, mas com efeito/ação hormonal semelhante. Nesse caso, moléculas com esse efeito são denominadas compostos com atividade hormono-similar (CASTILLO-ESPARZA et al., 2021; NARDI et al., 2002; SCAGLIA; POGNANI; ADANI, 2015).

A atividade auxino-similar é a influência de moléculas orgânicas da MO no metabolismo vegetal, semelhante ao efeito de uma auxina de fato, regulando, por exemplo, o crescimento da raiz, a absorção de nutrientes e, consequentemente, a produção vegetal (NARDI et al., 2002; SCAGLIA; POGNANI; ADANI, 2015).

Em estudos recentes, Wang et al. (2022) avaliaram a fitotoxicidade do hidrocarvão de resíduos de repolho por meio de testes de germinação, obtendo resultados positivos para o crescimento radicular. Sun et al. (2022) produziram hidrocarvão a partir de palha de junco e avaliaram sua influência no crescimento de mudas de amendoim em solo salino, relatando aumento do teor de hormônios nos tecidos vegetais. Bento et al. (2021) avaliaram o potencial bioestimulante do hidrocarvão de vinhaça na germinação de sementes de milho, indicando a presença de compostos fitotóxicos que inibiram a germinação das sementes.

Aminoácidos e ácidos orgânicos carboxílicos (ácido oxálico, tartárico e fenólico) foram relatados como apresentando efeitos semelhantes a auxinas quando testados como moléculas puras ou presentes como constituintes da fração orgânica (ou seja, matéria orgânica dissolvida ou alguma fração de substância húmica) (COLLA et al., 2014; PIZZEGHELLO et al., 2006; SINGH et al., 2014).

A complexidade química da MO dificulta a identificação analítica de moléculas semelhantes a auxinas que promovem o efeito de bioestimulação, e isso levou a tentativas de identificar quais das frações orgânicas que compõem a MO têm propriedades semelhantes a auxinas (CANELLAS et al., 2002; DELL'AGNOLA; NARDI, 1987; QUAGGIOTTI, 2004). Por exemplo, o fracionamento de ácidos húmicos em baixo peso molecular (HALMW) e alto peso molecular (HAHMW) e frações solúveis em água (WHA) (ZANDONADI et al., 2013), indicou que o peso molecular não afetou a atividade semelhante a auxina (DELL'AGNOLA; NARDI, 1987; MUSCOLO, 1999). Uma possível explicação para esse resultado consiste no fato de que os receptores de hormônio vegetal interagem com pequenas moléculas semelhantes a auxinas

presentes na MO e não com a MO total (CANELLAS et al., 2011; TREVISAN et al., 2010; ZANDONADI et al., 2013).

O objetivo deste trabalho foi avaliar o efeito auxino-similar do hidrocarvão preparado a partir de resíduos de milho, via carbonização hidrotérmica (HTC). Em particular, usando diferentes abordagens analíticas, ou seja, ATR-FTIR e Py-GC/MS, moléculas orgânicas responsáveis por efeitos bioestimulantes foram investigadas.

2. MATERIAIS E MÉTODOS

2.1. Produção do hidrocarvão

Este estudo foi realizado utilizando hidrocarvão preparado a partir de resíduo de milho.

As carbonizações hidrotérmicas (HTC) foram realizadas em um reator de Teflon revestido por titânio com volume de 100 mL. Os hidrocarvões foram preparados usando 1 g de resíduos de milho e 50 mL de água. O reator foi mantido a 200ºC em estufa (Sterilifer SX, São Caetano do Sul, Brasil) por 12 h. Essas condições foram previamente definidas por meio de um planejamento fatorial preliminar 2^3.

Os resíduos de milho foram coletados em um assentamento do Movimento dos Trabalhadores Rurais Sem Terra (MST), localizado no município de Serra Talhada, Pernambuco, Brasil (9°16'15.8"S 40°35'32.6"W). Os resíduos de milho foram coletados da parte aérea da planta, na forma de caule, folhas, palha e sabugo de milho. As matérias-primas frescas foram misturadas (com base no volume seco) e a proporção foi determinada pela combinação de cada resíduo na planta colhida: 81% caule e folhas, 10% palha e 9% sabugo de milho. A mistura foi triturada em moinho de facas e peneirada entre 500 e 250 mm. As seguintes análises foram realizadas com o objetivo de caracterizar a matéria-prima mista: matéria orgânica (MO) (NEN, 1994), carbono orgânico total (TOC) (utilisando analisador de carbono Sievers InnovOX – GE, Boulder, EUA) (NEN, 1994) e relações O/C e H/C (através análise elementar, utilizando um Perkin Elmer Series II CHNS/O Analyser 2400, Waltham, EUA).

Após a HTC, uma suspensão foi obtida e separada por filtração. A fração líquida (amostra LHC) foi armazenada a -4ºC e a fração sólida (amostra SHC) foi seca em estufa a 60ºC por 24 h, e então armazenada em dessecador. Testes de germinação foram realizados com a fração líquida do hidrocarvão (LHC) e com a matéria orgânica dissolvida (DOM), extraída da fração sólida (SHC). Os experimentos foram conduzidos no Laboratório de Química Ambiental (LQA) da Universidade Federal Rural de Pernambuco (UFRPE), Brasil.

2.2. Extração da matéria orgânica dissolvida (DOM)

A DOM foi extraída usando 5 g de hidrocarvão em um Erlenmeyer de 250 mL e 100 mL de água destilada. A amostra foi aquecida em banho Dubnoff a 40°C com agitação a 60 rpm por 30 min. Em seguida, o sobrenadante foi filtrado em sistema pressurizado, utilizando filtros de

acetato de celulose de 0,45 µm (Whatman), e armazenado em geladeira a -4°C (D'IMPORZANO; ADANI, 2007).

2.3. Caracterização do hidrocarvão

Os hidrocarvões líquido (LHC) e sólido (SHC) foram caracterizados em termos de carbono orgânico total (TOC) (usando um analisador de carbono Sievers InnovOX – GE, Boulder, EUA), razões O/C e H/C (via análise elementar, utilizando um Perkin Elmer Series II CHNS/O Analyser 2400, Waltham, EUA), pH (usando um medidor de pH Tecnal, Piracicaba, Brasil) e condutividade elétrica (EC) (usando um medidor de condutividade Tecnal Tec-4MP, Piracicaba, Brasil). Além disso, no hidrocarvão sólido (SHC) também foi determinado o teor de matéria orgânica (MO) (NEN, 1994).

2.4. Análise por MEV

O hidrocarvão (SHC) e o resíduos de milho foram analisados e comparados por Microscopia Eletrônica de Varredura (MEV). As amostras foram montadas em stubs de alumínio, com fita dupla face de carbono, colocadas sobre filme de papel alumínio e cobertas com ouro utilizando um metalizador DENTON VACUUM modelo DESKV (Moorestown, EUA). As micrografias foram obtidas em microscópio eletrônico de varredura TESCAN VEGA3 (Libušina, Chéquia).

2.5. Análise por ATR-FTIR

Os espectros na região do infravermelho foram obtidos a partir de um espectrofotômetro Shimadzu IR-Tracer 100 (Kyoto, Japão) e amostragem de Reflectância Total Atenuada (ATR) de desempenho de diamante/zinco seleneto e cristal, com resolução de 4 cm^{-1} e 16 acumulações. A região analisada variou entre 4000-600 cm^{-1}.

2.6. Caracterização por Py-GC/MS

A análise cromatográfica foi realizada em um Agilent 5975C Series GC/MSD (Santa Clara, EUA) e uma coluna capilar de 30,00 m × 250,00 µm × 0,25 µm ZB-Semivolatiles. O gás de arraste utilizado foi o He, injetado a uma vazão de 1,1 mL min^{-1}. Um volume de 1,0 µL de amostra foi injetado usando um injetor pirolisador (CDS 4000, Oxford, EUA) no modo splitless. O programa de temperatura foi ajustado para 60°C por 1 min e então aumentado para 325°C a uma taxa de 10°C min^{-1}. Os espectros de massa foram obtidos por impacto eletrônico a 70 eV e os dados coletados em uma faixa entre 50-660 m/Z. Os compostos foram identificados por comparação com espectros de massa da biblioteca Agilent Fiehn GC/MS Metabolomics RTL Library, usando o software AMDIS (software Automated Mass Spectral Deconvolution and Identification System, NIST 08).

Em relação ao LHC, a amostra foi primeiramente liofilizada para eliminar a água e assim concentrar o MO. Um liofilizador LabConco Benchtop (Kansas, EUA) foi usado no modo padrão durante 48 h.

2.7. Avaliação da atividade auxino-similar por bioensaios

A atividade auxino-similar do LHC e da DOM extraída do SHC foram avaliadas pela inibição do crescimento radicular de sementes de alface (*Lactuca sativa*, ISLA, Porto Alegre, Brasil). Os bioensaios foram preparados colocando 30 sementes em placas de Petri contendo papel filtro (Whatman 91) umedecido com 3,0 mL de água destilada (controle), ou 3,0 mL de solução da amostra nas seguintes concentrações:

LHC: 0,0557; 0,557; 5,57; 55,7; 348,125; 696,25; 1392,5; 2785,0 e 5570,0 mg C L^{-1}.

SHC: 0,026; 0,26; 2,6; 26,0; 162,5; 325,0; 650,0; 1300,0 e 2600,0 mg C L^{-1};

Para obtenção da curva de calibração foram realizados testes com 0,001, 0,004, 0,006, 0,01, 0,04, 0,06, 0,1 e 0,2 mg C L^{-1} de auxina (ácido 3-indolacético-AIA, Sigma Aldrich, I3750). As sementes foram germinadas no escuro a 25°C; após 5 dias, as mudas foram removidas e os comprimentos das raízes medidos (PIZZEGHELLO et al., 2006).

O comprimento da raiz foi definido a partir da ponta da raiz até o ponto onde a radícula emergiu do tegumento. Comprimentos de raiz abaixo de 5 mm foram considerados sementes não germinadas (PIZZEGHELLO et al., 2006; WANG et al., 2001).

Os dados foram apresentados como um índice de comprimento (LI), calculado pela divisão do comprimento médio da amostra e a média do comprimento obtido no controle.

A atividade hormono-similar foi considerada presente quando a tendência LI vs. [C] foi estatisticamente significativa (Sig. <0,05) e seguiu uma curva logarítmica (ERTANI et al., 2013; PIZZEGHELLO et al., 2006).

2.8. Análises estatísticas

A análise de variância ANOVA One-Way foi usada para avaliar as diferenças entre as médias para $p < 0,01$, usando testes de intervalo múltiplo de Duncan. A regressão linear bootstrap foi aplicada para determinar a relação do efeito semelhante ao hormônio versus a dose de moléculas bioestimulantes. O software IBM SPSS Statistics v. 29 foi usado para análise de dados.

3. RESULTADOS E DISCUSSÃO

3.1. Caracterização do hidrocarvão

As características químicas dos hidrocarvões são apresentadas na Tabela 1. A partir da observação desses parâmetros, é possível acompanhar o efeito da carbonização hidrotérmica na evolução da MO, ou seja, mudanças na cor e no tamanho das partículas (textura), além de um aumento significativo do TOC e uma pequena diminuição da MO (Tabela 1).

O hidrocarvão sólido apresentou coloração preta, diferente do tom amarelado apresentado pelo resíduo de milho, indicando a carbonização da MO. Outra observação diz respeito às partículas de menor tamanho, obtidas na forma de pó no hidrocarvão, diferentes quando comparadas ao resíduo fresco (500-250 mm). Mudanças na cor e no tamanho das partículas são evidências do alto grau de carbonização da biomassa (SANTANA et al., 2022). Com base em testes preliminares, HTC mais longa (mais de 10 h) e temperaturas mais altas (máximo de 200°C permitido pelo Teflon) favoreceram o processo. Neste caso, o rendimento médio foi de 57,35% (m/m). A fusão de moléculas orgânicas e a solubilização de alguns compostos em água contribuíram para diminuir o rendimento do hidrocarvão (SHC) (FAROBIE et al., 2022; VENKATESAN et al., 2022; ZHANG et al., 2019). Por outro lado, as cadeias fundidas enriqueceram a fração líquida com compostos orgânicos, conforme observado. O rendimento médio da fração líquida (LHC) foi de 17%. Apenas a HTC acima de 180° originou a fração líquida.

O TOC aumentou 52% no SHC quando comparado ao resíduo de milho. A MO diminuiu 6,4%. Alterações no teor de carbono estão relacionadas principalmente a quebras de (macro)moléculas, além de processos de desidratação, descarboxilação e a consequente condensação e aromatização das cadeias de carbono, concentrando o carbono orgânico no hidrocarvão (LI; CAI, 2022; WANG et al., 2020).

Reduções significativas na relação H/C e no O/C também indicaram o alto grau de transformação da MO durante o processo de HTC. A relação H/C reduziu de 0,18 na matéria-prima para 0,08 na hidrocarvão (76% de diferença). A relação O/C passou de 0,81 para 0,21 (117% de diferença). Ambas as razões são estatisticamente diferentes entre si de acordo com ANOVA One-way e o teste de Duncan em $p < 0,05$.

A relação H/C é um parâmetro importante recomendado para determinar a qualidade do hidrocarvão. Em geral, a relação H/C muda substancialmente quando um tratamento termoquímico é eficiente, e valores abaixo de 0,7 são recomendados. Além disso, a relação O/C está correlacionada com a estabilidade do hidrocarvão. A relação H/C é uma propriedade correlacionada com o grau de alteração termoquímica que produz estruturas de anéis aromáticos fundidos no hidrocarvão. A presença dessas estruturas é uma medida intrínseca da estabilidade molecular (PEREIRA et al., 2011; SEVILLA; FUERTES, 2009; SPOKAS, 2010). Os resultados obtidos concordaram com a literatura que relatou baixas rações de H/C e O/C após o processo de HTC (ARAGÓN-BRICEÑO et al., 2020; SANTANA et al., 2022; SEVILLA; FUERTES, 2009).

Tabela 1. Caracterização química do resíduo de milho e do hidrocarvão líquido/sólido.

	Resíduo de milho[c]	SHC[c]	SHC/DOM[ac]	LHC
MO[a] (%)	97,19 ± 0,11b	91,35 ± 0,26a	-	-
TOC[ab]	43,32 ± 0,00a	73,13 ± 0,00b	2,60 ± 0,00	5,57 ± 0,00
pH	-	-	4,55 ± 0,01b	3,71 ± 0,00a
EC (µS cm^{-1})	-	-	2,90 ± 0,03a	3,84 ± 0,00b
Análise elementar				
H (%)	7,79 ± 0,01b	5,85 ± 0,02b	5,52 ± 0,02b	4,19 ± 0,02a
N (%)	3,12 ± 0,00b	3,39 ± 0,01b	2,02 ± 0,02a	2,99 ± 0,02a
O (%)	35,08 ± 0,04c	15,35 ± 0,03a	16,32 ± 0,02ab	20,85 ± 0,08b
Razão molar				
O/C[d]	0,81 ± 0,01b	0,21 ± 0,01a	-	-
H/C[d]	0,18 ± 0,00b	0,08 ± 0,00a	-	-

[a] MO = Matéria orgânica particulada; TOC = Carbono orgânico total.

[b] Unidade de TOC: Resíduo de milho SHC em %; LHC e SHC/DOM em g L^{-1}. Os valores de TOC foram usados para calcular as razões O/C e H/C.

[c] Valores na mesma linha seguidos da mesma letra não são estatisticamente diferentes um do outro, em $p < 0,05$ de acordo com ANOVA One-way e teste de Duncan.

[d] O desvio padrão de O/C e H/C foi calculado como: $std = O/C \times [(std\ O \div O)^2 + (std\ C \div C)^2]^{1/2}$ e $std = H/C \times [(std\ H \div H)^2 + (std\ C \div C)^2]^{1/2}$.

3.2. Análise por MEV

As micrografias do MEV são mostradas na Figura 1. Três micrografias são apresentadas nas escalas de 10, 50 e 100 μm, comparando-se as superfícies do resíduo de milho e da amostra SHC. A imagem microscópica indicou como a carbonização hidrotérmica atuou sobre a matéria-prima, alterando o material pela abertura de poros e ranhuras.

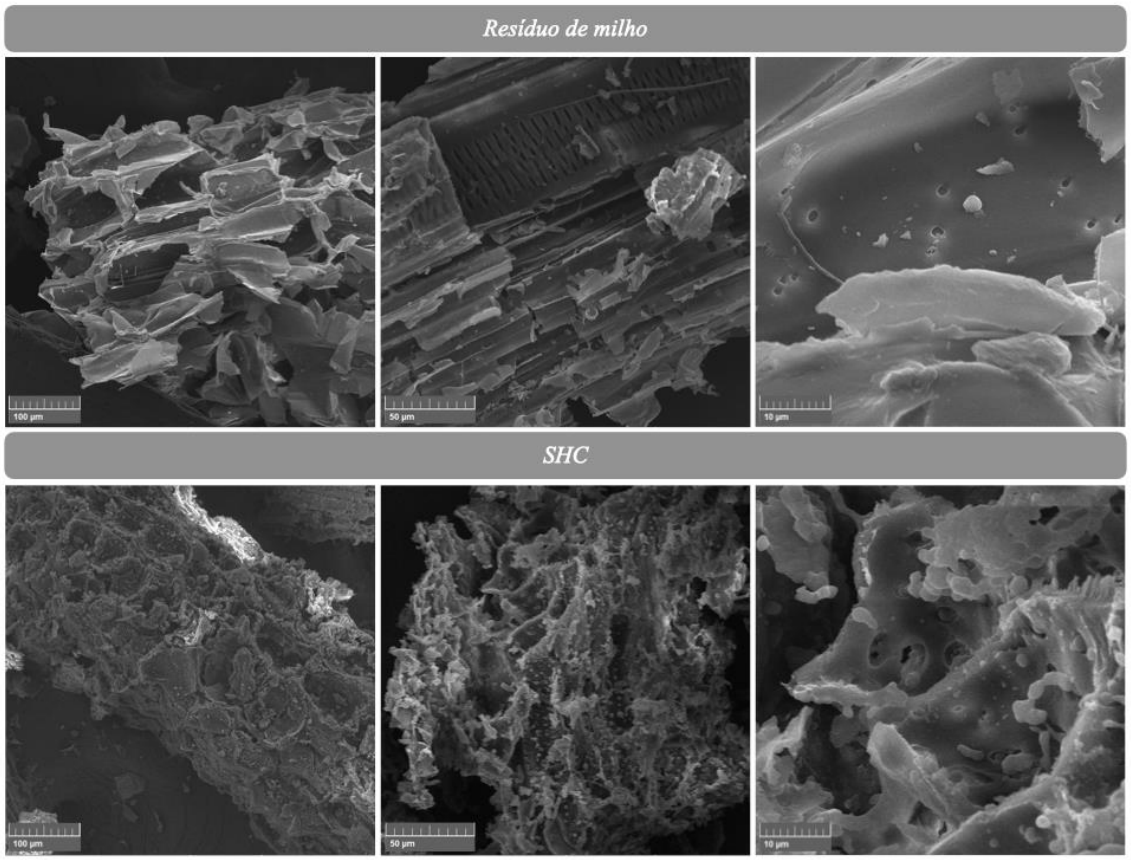

Figura 1. Morfologia da superfície do resíduo de milho e hidrocarvão por MEV.

Poros com nano dimensão não foram identificados por MEV com ampliação de 1.000X. No entanto, a presença de poros estruturados foi confirmada, aumentando assim a área superficial do hidrocarvão e, consequentemente, favorecendo a retenção de íons, umidade e compostos orgânicos.

A HTC também tornou a superfície do hidrocarvão mais áspera, quando comparado com os resíduos de milho. Essa mudança superficial foi mais evidente nas escalas de 100 e 50 μm. Além disso, a distribuição das cavidades é aparentemente homogênea ao longo da estrutura do hidrocarvão. Este aspecto é essencial para promover a maior área superficial e capacidade de adsorção.

3.3. Análise por ATR-FTIR

Os espectros do ATR-FTIR são mostrados na Figura 2. Em geral, cada espectro é significativamente diferente um do outro e indicou como os grupos moleculares/funcionais foram alterados durante o HTC, quando os resíduos de milho foram convertidos em hidrocarvão (SHC e LHC).

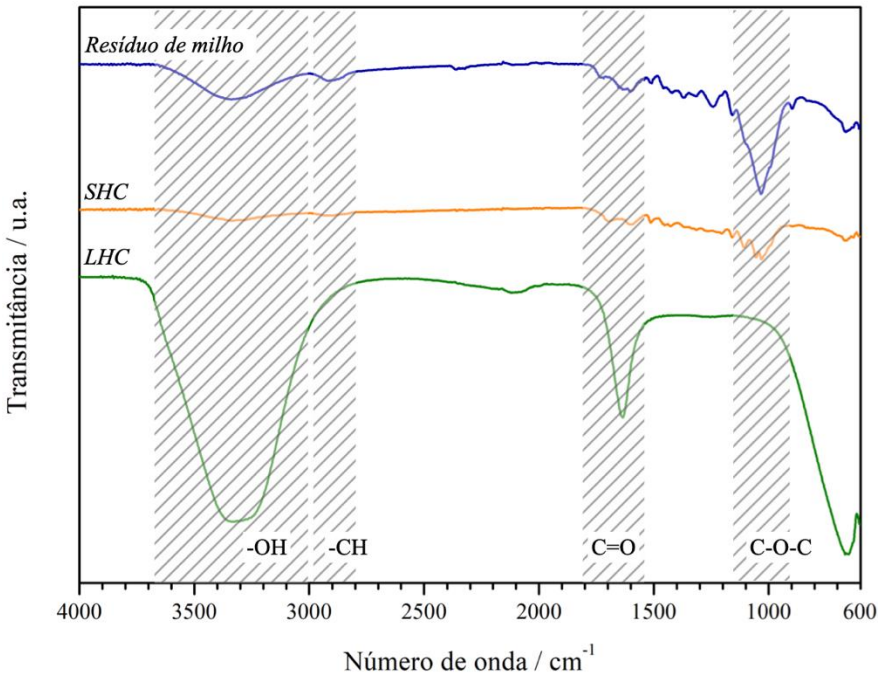

Figura 2. Espectro ATR-FTIR de resíduos de milho e hidrocarvões (LHC e SHC).

A banda em 3300 cm^{-1} nos resíduos de milho foi atribuída principalmente às vibrações de alongamento -OH presentes na água e nos polissacarídeos, tem baixa intensidade no SHC, indicando a desidratação da matéria-prima devido ao aumento da temperatura na HTC, além da quebra das moléculas de polissacarídeos. No LHC, a água da fase aquosa do hidrocarvão intensifica essa banda, indicando também a presença de grupos hidroxila dissolvidos e compostos fenólicos (SANTANA et al., 2022).

A região entre 3000 e 2800 cm^{-1} nos resíduos de milho está associada às ligações $-CH_3$, $-CH_2$ e CH e diminui após a HTC na amostra SHC. (FAROBIE et al., 2022; SANTANA et al., 2022)

Na região entre 1700 e 1400 cm^{-1}, as bandas observadas nos resíduos de milho estão associadas a grupos funcionais contendo C=O. Essas bandas são de menor intensidade no SHC, indicando que as reações de descarboxilação ocorreram durante o processo HTC (FAROBIE et al., 2022; SANTANA et al., 2022; WANG et al., 2020).

A banda em 1600 cm^{-1} no LHC é atribuída ao alongamento das ligações C=C e C-H em compostos aromáticos, enquanto a faixa a 690 cm^{-1} está associada principalmente a deformações angulares de anéis aromáticos, indicando a forte natureza aromática da fração líquida (LIU et al., 2021; ZHANG et al., 2019).

A banda presente nos resíduos de milho a 1000 cm^{-1} está associada ao alongamento das ligações C-O e C-O-C em polissacarídeos, como a celulose. No SHC esta intensidade diminuiu, indicando degradação da celulose pela alta temperatura e pressão durante a HTC (FAROBIE et al., 2022; SANTANA et al., 2022; WANG et al., 2020).

3.4. Atividade auxino-similar dos hidrocarvões

Os hidrocarvões sólido e líquido foram testados para propriedades auxino-similares (AIA-similar). O hidrocarvão sólido foi testado em termos de DOM extraída. Os resultados dos bioensaios indicaram que ambas as formas tinham atividade semelhante a hormônio (Tabelas 2 e 3). O LHC inibiu o crescimento de todas as raízes nas maiores concentrações, acima de 696,25 mg C L^{-1}. No entanto, SHC inibiu parcialmente em todas as concentrações, sem inibir completamente o crescimento radicular, mesmo na concentração mais alta. Este resultado era esperado, uma vez que a diferença de carbono foi significativa entre as amostras (Tabela 1). Os resultados obtidos concordam com a literatura que relatou atividade semelhante a AIA para hidrocarvões (BENTO et al., 2020; EGAMBERDIEVA et al., 2020; MASSAYA; MILLS-LAMPTEY; CHUCK, 2022; SUN et al., 2022).

Os testes de bioensaios foram realizados em uma ampla faixa de concentração de carbono (0,026 – 2600 mg C L^{-1} para SHC e 0,0557 – 5570 mg C L^{-1} para LHC). No entanto, a atividade AIA-similar foi verificada para o SHC na faixa de concentração 26 – 2600 mg C L^{-1}, e 5,57 – 5570 mg C L^{-1} para o LHC. Em outras palavras, a atividade AIA-similar foi verificada a partir de 1% e 0,1% da concentração total de C, respectivamente. O coeficiente angular da curva logarítmica (LI/[C]) foi usado para avaliar a intensidade da atividade AIA-similar (SCAGLIA; POGNANI; ADANI, 2015), obtendo a seguinte escala: SHC < LHC (Tabela 3). O efeito semelhante ao AIA mais eficaz foi encontrado para o LHC, sugerindo que a fusão de moléculas mais lábeis aumentou o desenvolvimento da atividade AIA-similar como consequência da transformação ocorrida durante o processo de HTC.

Tabela 2. Índice de comprimento (LI) das raízes de *Lactuca sativa* após a aplicação de hidrocarvões líquidos e sólidos e do ácido 3-indolacético (AIA).

SHC		LHC		AIA	
Doses da DOM (mg C L^{-1})	LI (índice de comprimento)	Doses (mg C L^{-1})	LI	Doses (mg C L^{-1})	LI
26	0,91 ± 0,06abc [a]	5,57	0,90 ± 0,03bc	0,001	0,49 ± 0,22d
162,5	0,85 ± 0,07abc	55,7	0,76 ± 0,06bc	0,004	0.28 ± 0,06c
325	0,85 ± 0,08abc	348,125	0,77 ± 0,07bc	0,006	0,11 ± 0,02b
650	0,67 ± 0,60abc	696,25	0,71 ± 0,05b	0,01	0,06 ± 0,01a
1300	0,67 ± 0,01ab	1392,5	0,00 ± 0,00a	0,04	0,04 ± 0,01a
2600	0,62 ± 0,06a	2785	0,00 ± 0,00a	0,06	0,04 ± 0,04a
-	-	5570	0,00 ± 0,00a	0,1	0,02 ± 0,02a

[a] Valores na mesma coluna seguidos da mesma letra não são estatisticamente diferentes um do outro para $p < 0,05$, de acordo com os testes ANOVA One-way e Duncan.

Tabela 3. Atividade hormono-similar (efeito AIA-similar) observada em bioensaios com hidrocarvão líquido e sólido e ácido 3-indolacético (AIA).

	Intervalo de atividade AIA-similar (mg C L^{-1})	Equação do efeito AIA-similar	R^2	Sig.
SHC[a]	26,0-2600,0 mg C $^{L-1}$	$y = -0{,}068 \times ln(x) + 1{,}168$	0,856	0,022
LHC	5,57-5570,0 mg C $^{L-1}$	$y = -0{,}146 \times ln(x) + 1{,}323$	0,687	0,001
AIA	0,001-0,01 mg C $^{L-1}$	$y = -0{,}193 \times ln(x) - 0{,}834$	0,962	0,019

[a] Hidrocarvão sólido foi testado na forma de matéria orgânica dissolvida (DOM) extraída.

3.5. Caracterização por Py-GC/MS

Os resultados discutidos acima indicaram a presença de atividade hormonal nos hidrocarvões sólido e líquido.

A abordagem Py-GC/MS confirmou informações importantes sobre a presença e a quantidade de moléculas específicas contidas no SHC e LHC. Agora ela pode ser usada para elucidar quais moléculas foram responsáveis pelo efeito bioestimulante.

A DOM extraída do SHC e o LHC foram caracterizados por diferentes classes de moléculas como monossacarídeos, aminoácidos, nucleotídeos, ácidos carboxílicos lineares e aromáticos, alfa-hidroxiácidos e alditóis (Tabela S1).

Em geral, LHC e SHC apresentaram aproximadamente a mesma concentração de compostos orgânicos, divididos em classes moleculares, totalizando 358,01 ± 12,33 μg g^{-1} no LHC e 300,26 ± 11,91 μg g^{-1} no SHC. Diferenças estatísticas foram observadas apenas nas seguintes classes: nucleotídeos, alditóis, ácidos carboxílicos aromáticos e aminoácidos (ANOVA bootstrap, $p < 0,05$); no entanto, nenhuma diferença entre as classes moleculares excedeu 18%. Por outro lado, o DOM extraída do SHC apresentou um total de 124,84 ± 21,91 μg g^{-1} de compostos orgânicos, soma consideravelmente abaixo dos resultados de LHC e SHC, também estatisticamente diferente em todas as classes moleculares (ANOVA bootstrap, $p < 0,05$) (Figura 3).

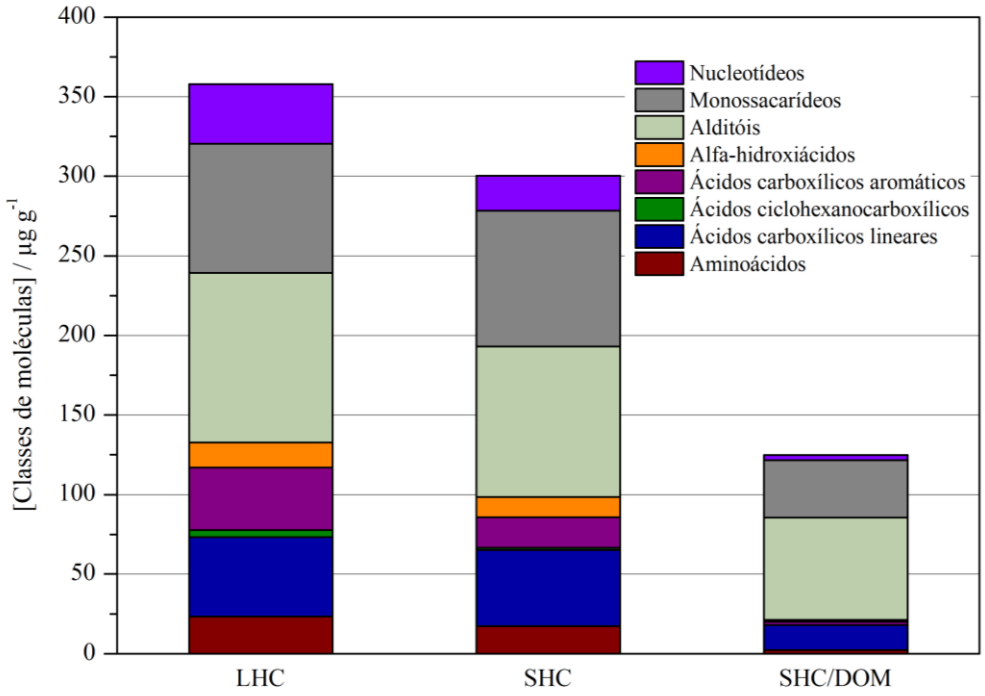

Figura 3. Moléculas orgânicas detectadas nos hidrocarvões e na DOM por Py-GC/MS.

A Tabela S1 e a Figura 3 indicam por que, embora ambas as amostras tenham atividade semelhante à auxina (Tabela 3), os efeitos observados nos testes de germinação com LCH e SHC/DOM são tão diferentes. Compostos como alfa-hidroxiácidos, ácidos carboxílicos aromáticos, nucleotídeos e aminoácidos foram quantificados entre 0 e 3,38 ± 0,11 μg g^{-1} em SHC/DOM.

Em particular, os ácidos carboxílicos (aromáticos e lineares) e os aminoácidos têm sido relatados por muitos estudos como tendo efeitos AIA-similar (COLLA et al., 2014; ERTANI et al., 2009; PIZZEGHELLO et al., 2006; SINGH et al., 2014; TREVISAN et al., 2010). Uma alta presença de grupos carboxílicos foi correlacionada com o efeito auxina (TREVISAN et al., 2010). Além disso, aminoácidos foram relatados por efeitos fortes ou fracos semelhantes ao AIA, dependendo da presença de triptofano (o precursor metabólico do AIA) ou, geralmente, pela concentração de aminoácidos (COLLA et al., 2014; ERTANI et al., 2009). Além disso, a eficácia do efeito AIA-similar também foi diretamente associada à concentração de ácidos carboxílicos aromáticos específicos (ou seja, vanilina, ácido ferúlico, ácido protocatecuico, ácido 4-hidroxibenzoico e ácido 4-hidroxicinâmico) (FERRO et al., 2006; PIZZEGHELLO et al., 2006; SINGH et al., 2014).

No entanto, a complexa composição química relatada na Tabela S1 não permitiu explicar claramente o efeito bioestimulante do SHC e do LHC, uma vez que moléculas bioestimulantes estavam presentes nas amostras estudadas. No entanto, muitos autores relataram que apenas a presença de moléculas específicas não é suficiente para obter efeitos estimulantes, uma vez que a concentração molecular e a biodisponibilidade também desempenham papéis importantes. Já levando-se em consideração a concentração total no LHC e SHC/DOM (amostras aplicadas nos testes de germinação) de moléculas com atividade semelhante a AIA, cada classe teve sua soma de concentração, ou seja, ácidos carboxílicos e aminoácidos (Tabela S1), e o efeito comparado entre as amostras, associando o grupo mais relatado de classes moleculares que apresenta efeito AIA-similar (Figura 4). No LHC, a soma da concentração de moléculas ativas foi de 112,36 ± 3,58 μg g^{-1} (intervalo de concentração entre 23,26 ± 4,81 μg g^{-1} e 50,14 ± 3,62 μg g^{-1}) e na concentração de moléculas ativas SHC foi de 20,29 ± 2,92 μg g^{-1} (intervalo de concentração entre 2,22 ± 0,69 μg g^{-1} e 15,85 ± 0,42 μg g^{-1}).

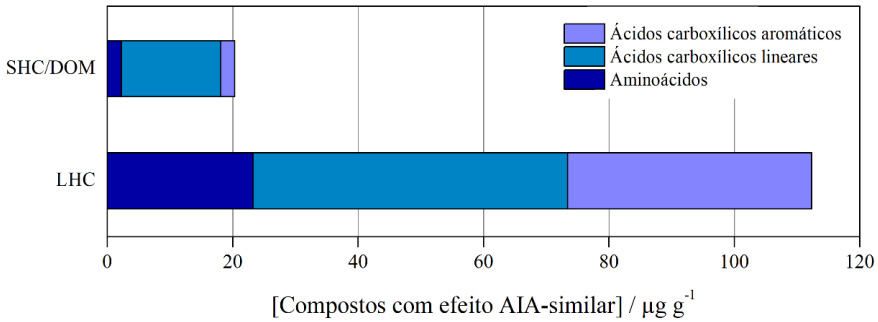

Figura 4. Compostos AIA-similar em LHC e SHC/DOM determinados por Py-GC/MS.

Os conteúdos de compostos com efeito AIA-similiar foram estatisticamente diferentes para SHC/DOM e LHC (ANOVA bootstrap, $p < 0,05$), sugerindo que uma maior concentração de moléculas bioestimulantes resultou em uma atividade bioestimulante mais eficaz. Mesmo com um resultado menor em SHC/DOM, os resultados indicaram que, mesmo em baixas concentrações de compostos AIA-similares, foi observado um efeito bioestimulante, conforme relatado na Tabela 2. Assim, mesmo em baixas concentrações, o hidrocarvão sólido pode ser considerado bioativo e pode influenciar positivamente o desenvolvimento da planta, conforme demonstrado nos testes de germinação. Essa hipótese foi corroborada pela ótima regressão linear encontrada entre o coeficiente linear e a concentração de compostos AIA-similares (Tabela 3). De qualquer forma, levando em consideração o que foi discutido acima e os dados relatados na Figura 3, pode-se concluir que uma concentração de moléculas bioestimulantes de 20 µg g^{-1} pode ser indicada como o limite acima do qual um efeito bioestimulante mais intenso iniciou.

4. CONCLUSÃO

O hidrocarvão preparado a partir de resíduos de milho foi testado para atividade hormono-similar (efeito auxina). Os resultados obtidos indicaram que a carbonização hidrotérmica afetou essa atividade, concentrando e/ou produzindo ácidos carboxílicos (aromáticos e lineares) e aminoácidos, sendo essas moléculas as sugeridas como responsáveis pela atividade hormono-similar. O hidrocarvão líquido foi consideravelmente mais bioativo do que a matéria orgânica dissolvida extraída do hidrocarvão sólido, inclusive apresentando efeito auxino-similar nos testes de germinação. Uma concentração total de moléculas de 20 µg g^{-1} foi mostrada como uma concentração limite acima da qual elas produziram uma atividade bioestimulante mais intensa.

REFERÊNCIAS

ARAGÓN-BRICEÑO, C. I. et al. Hydrothermal carbonization of sewage digestate at wastewater treatment works: Influence of solid loading on characteristics of hydrochar, process water and plant energetics. **Renewable Energy**, v. 157, p. 959–973, 2020.

AWOGBEMI, O.; KALLON, D. V. VON. Valorization of agricultural wastes for biofuel applications. **Heliyon**, v. 8, n. 10, p. 1–16, 2022.

AYODELE, O. O. et al. Application of biomass-derived hydrochar in process stability of anaerobic digestion. **Bioresource Technology Reports**, v. 17, n. 100903, p. 1–8, 2022.

BENTO, L. R. et al. Release of nutrients and organic carbon in different soil types from hydrochar obtained using sugarcane bagasse and vinasse. **Geoderma**, v. 334, p. 24–32, 2019.

BENTO, L. R. et al. Humic extracts of hydrochar and Amazonian Dark Earth: Molecular characteristics and effects on maize seed germination. **Science of The Total Environment**, v. 708, n. 135000, p. 1–11, 2020.

BENTO, L. R. et al. Hydrochar obtained with by-products from the sugarcane industry: Molecular features and effects of extracts on maize seed germination. **Journal of Environmental Management**, v. 281, n. 111878, p. 1–12, 2021.

CANELLAS, L. P. et al. Humic Acids Isolated from Earthworm Compost Enhance Root Elongation, Lateral Root Emergence, and Plasma Membrane H+-ATPase Activity in Maize Roots. **Plant Physiology**, v. 130, n. 4, p. 1951–1957, 2002.

CANELLAS, L. P. et al. Probing the hormonal activity of fractionated molecular humic components in tomato auxin mutants. **Annals of Applied Biology**, v. 159, n. 2, p. 202–211, 2011.

CASTILLO-ESPARZA, J. F. et al. Pisolithus tinctorius extract affects the root system architecture through compound production with auxin-like activity in Arabidopsis thaliana. **Rhizosphere**, v. 19, n. 100397, p. 1–7, 2021.

CHEN, N. et al. Structural dependent Cr(VI) adsorption and reduction of biochar: hydrochar versus pyrochar. **Science of The Total Environment**, v. 783, n. 147084, p. 1–11, 2021.

COLLA, G. et al. Biostimulant action of a plant-derived protein hydrolysate produced through enzymatic hydrolysis. **Frontiers in Plant Science**, v. 5, n. 448, p. 1–6, 2014.

DELL'AGNOLA, G.; NARDI, S. Hormone-like effect and enhanced nitrate uptake induced by depolycondensed humic fractions obtained from Allolobophora rosea and A. caliginosa faeces. **Biology and Fertility of Soils**, v. 4, n. 3, p. 115–118, jun. 1987.

D'IMPORZANO, G.; ADANI, F. The contribution of water soluble and water insoluble organic fractions to oxygen uptake rate during high rate composting. **Biodegradation**, v. 18, n. 1, p. 103–113, 2007.

EGAMBERDIEVA, D. et al. The Effect of Biochars and Endophytic Bacteria on Growth and Root Rot Disease Incidence of Fusarium Infested Narrow-Leafed Lupin (Lupinus angustifolius L.). **Microorganisms 2020, Vol. 8, Page 496**, v. 8, n. 4, p. 1–16, 2020.

ERTANI, A. et al. Biostimulant activity of two protein hydrolyzates in the growth and nitrogen metabolism of maize seedlings. **Journal of Plant Nutrition and Soil Science**, v. 172, n. 2, p. 237–244, 1 abr. 2009.

ERTANI, A. et al. Humic-like substances from agro-industrial residues affect growth and nitrogen assimilation in maize (Zea mays L.) plantlets. **Journal of Geochemical Exploration**, v. 129, p. 103–111, 2013.

FAROBIE, O. et al. Simultaneous production of nutritional compounds and hydrochar from Chlorella pyrenoidosa via hydrothermal process. **Bioresource Technology Reports**, v. 20, n. 101245, p. 1–9, 2022.

FERRO, N. et al. Coulomb and overlap self-similarities: a comparative selectivity analysis of structure-function relationships for auxin-like molecules. **Journal of chemical information and modeling**, v. 46, n. 4, p. 1751–1762, 2006.

HARIS, M. et al. Synthesis of functional hydrochar from olive waste for simultaneous removal of azo and non-azo dyes from water. **Chemical Engineering Journal Advances**, v. 9, n. 100233, p. 1–10, 2022.

HOU, P. et al. Win-win: Application of sawdust-derived hydrochar in low fertility soil improves rice yield and reduces greenhouse gas emissions from agricultural ecosystems. **Science of The Total Environment**, v. 748, n. 142457, p. 1–9, 2020.

IGHALO, J. O. et al. Recent advances in hydrochar application for the adsorptive removal of wastewater pollutants. **Chemical Engineering Research and Design**, v. 184, p. 419–456, ago. 2022.

KANG, K. et al. Microwave-assisted hydrothermal carbonization of corn stalk for solid biofuel production: Optimization of process parameters and characterization of hydrochar. **Energy**, v. 186, n. 115795, p. 1–11, 2019.

KAVINDI, G. A. G. et al. Use of hydrochar from hydrothermal co-carbonization of rice straw and sewage sludge for Cr(VI) bioremediation in soil. **Bioresource Technology Reports**, v. 18, n. 101052, p. 1–8, jun. 2022.

KHOSRAVI, A. et al. Production and characterization of hydrochars and their application in soil improvement and environmental remediation. **Chemical Engineering Journal**, v. 430, n. 133142, p. 1–20, 2022.

LANG, J. et al. Evaluation and selection of biochars and hydrochars derived from agricultural wastes for the use as adsorbent and energy storage materials. **Journal of Environmental Chemical Engineering**, v. 9, n. 5, p. 1–17, 2021.

LANG, Q. et al. Combustion characteristics, kinetic and thermodynamic analyses of hydrochars derived from hydrothermal carbonization of cattle manure. **Journal of Environmental Chemical Engineering**, v. 10, n. 1, p. 1–10, 2022.

LI, C.; CAI, R. Preparation of solid organic fertilizer by co-hydrothermal carbonization of peanut residue and corn cob: A study on nutrient conversion. **Science of The Total Environment**, v. 838, n. 155867, p. 1–12, 2022.

LIN, H. et al. Hydrothermal carbonization of cellulose in aqueous phase of bio-oil: The significant impacts on properties of hydrochar. **Fuel**, v. 315, n. 123132, p. 1–13, 2022.

LIU, Q. et al. Fast hydrothermal co-liquefaction of corn stover and cow manure for biocrude and hydrochar production. **Bioresource Technology**, v. 340, n. 125630, p. 1–11, 2021.

MARIUZZA, D. et al. Impact of Co-Hydrothermal carbonization of animal and agricultural waste on hydrochars' soil amendment and solid fuel properties. **Biomass and Bioenergy**, v. 157, n. 106329, p. 1–12, 2022.

MASSAYA, J.; MILLS-LAMPTEY, B.; CHUCK, C. J. Soil Amendments and Biostimulants from the Hydrothermal Processing of Spent Coffee Grounds. **Waste and Biomass Valorization**, v. 13, n. 6, p. 2889–2904, 2022.

MOHAMMADI, A. et al. Effects of wood ash on physicochemical and morphological characteristics of sludge-derived hydrochar pellets relevant to soil and energy applications. **Biomass and Bioenergy**, v. 163, n. 106531, p. 1–10, ago. 2022.

MUSCOLO, A. Earthworm humic matter produces auxin-like effects on Daucus carota cell growth and nitrate metabolism. **Soil Biology and Biochemistry**, v. 31, n. 9, p. 1303–1311, 1999.

NARDI, S. et al. Physiological effects of humic substances on higher plants. **Soil Biology and Biochemistry**, v. 34, n. 11, p. 1527–1536, 2002.

NEN 5754. Determination of organic matter content in soil as loss-on-ignition. **Netherlands Normalisation Institute**, 1994.

PEREIRA, C. R. et al. Contribution to characterisation of biochar to estimate the labile fraction of carbon. **Organic Geochemistry**, v. 42, n. 11, p. 1331–1342, 2011.

PIZZEGHELLO, D. et al. Chemical and biological characterization of dissolved organic matter from silver fir and beech forest soils. **Chemosphere**, v. 65, n. 2, p. 190–200, 2006.

QUAGGIOTTI, S. Effect of low molecular size humic substances on nitrate uptake and expression of genes involved in nitrate transport in maize (Zea mays L.). **Journal of Experimental Botany**, v. 55, n. 398, p. 803–813, 2004.

QUEVEDO-AMADOR, R. A. et al. Functionalized hydrochar-based catalysts for biodiesel production via oil transesterification: Optimum preparation conditions and performance assessment. **Fuel**, v. 312, n. 122731, p. 1–11, 2022.

SANTANA, M. S. et al. Structural, inorganic, and adsorptive properties of hydrochars obtained by hydrothermal carbonization of coffee waste. **Journal of Environmental Management**, v. 302, n. 114021, p. 1–11, 2022.

SCAGLIA, B.; POGNANI, M.; ADANI, F. Evaluation of hormone-like activity of the dissolved organic matter fraction (DOM) of compost and digestate. **Science of the Total Environment**, v. 514, p. 314–321, 2015.

SEVILLA, M.; FUERTES, A. B. The production of carbon materials by hydrothermal carbonization of cellulose. **Carbon**, v. 47, p. 2281–2289, 2009.

SHUANG, E. et al. Engineering functional hydrochar based catalyst with corn stover and model components for efficient glucose isomerization. **Energy**, v. 249, n. 123668, p. 1–11, jun. 2022.

SINGH, H. P. et al. Ferulic acid impairs rhizogenesis and root growth, and alters associated biochemical changes in mung bean (*Vigna radiata*) hypocotyls. **Journal of Plant Interactions**, v. 9, n. 1, p. 267–274, 2014.

SPOKAS, K. A. Review of the stability of biochar in soils: Predictability of O:C molar ratios. **Carbon Management**, v. 1, n. 2, p. 289–303, 2010.

SUN, R. et al. Comparative study of pyrochar and hydrochar on peanut seedling growth in a coastal salt-affected soil of Yellow River Delta, China. **Science of The Total Environment**, v. 833, n. 155183, p. 1–11, 2022.

TREVISAN, S. et al. Humic substances biological activity at the plant-soil interface. **Plant Signaling & Behavior**, v. 5, n. 6, p. 635–643, 2010.

USDA - UNITED STATES DEPARTMENT OF AGRICULTURE. **Foreign Agricultural Service. Production, Supply and Distribution**. Disponível em: <https://apps.fas.usda.gov/psdonline/app/index.html#/app/advQuery>. Acesso em: 14 nov. 2022.

VENKATESAN, S. et al. Evaluation of the production of hydrochar from spent coffee grounds under different operating conditions. **Journal of Water Process Engineering**, v. 49, n. 103037, p. 1–14, 2022.

WANG, G. et al. Hydrothermal carbonization of maize straw for hydrochar production and its injection for blast furnace. **Applied Energy**, v. 266, n. 114818, p. 1–11, 2020.

WANG, M. et al. Hydrothermal conversion of Chinese cabbage residue for sustainable agriculture: Influence of process parameters on hydrochar and hydrolysate. **Science of The Total Environment**, v. 812, n. 152478, p. 1–9, mar. 2022.

WANG, X. et al. Validation of germination rate and root elongation as indicator to assess phytotoxicity with Cucumis sativus. **Chemosphere**, v. 44, n. 8, p. 1711–1721, 2001.

ZANDONADI, D. B. et al. Plant physiology as affected by humified organic matter. **Theoretical and Experimental Plant Physiology**, v. 25, n. 1, p. 12–25, 2013.

ZHANG, Y. et al. Effects of temperature, time and acidity of hydrothermal carbonization on the hydrochar properties and nitrogen recovery from corn stover. **Biomass and Bioenergy**, v. 122, p. 175–182, 2019.

ZHANG, Y.; QIN, J.; YI, Y. Biochar and hydrochar derived from freshwater sludge: Characterization and possible applications. **Science of the Total Environment**, v. 763, n. 144550, p. 1–8, 2021.

APÊNDICE

APÊNDICE A – MATERIAL SUPLEMENTAR

Tabela S1. Caracterização Py-GC/MS do hidrocarvão sólido e líquido (SHC e LHC) e da DOM extraída do SHC (média ± DP, n = 3, com base na matéria seca).

Classes de moléculas		**LHC**	**SHC**	**DOM/SHC**	**Efeito AIA-similar**
			μg g^{-1} (m/m)		
Aminoácidos	L-Serina	3,15 ± 0,08	2,52 ± 0,27	0	Colla et al., 2014
	Ácido L-glutâmico (desidratado)	4,93 ± 0,43	5,43 ± 0,60	1,24 ± 0,03	Ertani et al., 2009
	Ácido L-piroglutâmico	15,18 ± 1,02	9,32 ± 0,02	0,98 ± 0,11	
Ácidos carboxílicos lineares	Ácido glicólico	9,24 ± 0,33	11,46 ± 1,01	1,24 ± 0,53	Trevisan et al., 2010
	L-(+) Ácido lático	5,27 ± 0,41	4,68 ± 0,44	0,07 ± 0,00	
	Ácido oxálico	8,82 ± 0,94	8,36 ± 0,74	4,54 ± 0,48	
	Ácido succínico	11,44 ± 0,74	5,33 ± 0,59	0	
	Ácido cítrico	15,37 ± 0,98	18,27 ± 1,20	10,00 ± 0,74	
Ácidos ciclohexanocarboxílicos	Ácido quínico	4,49 ± 0,56	1,25 ± 0,01	0	
Ácidos carboxílicos aromáticos	Ácido 4-hidroxi-3-metoxibenzoico	10,71 ± 0,11	2,35 ± 0,03	0	*Vanilina-similar:*
	Ácido 4-hidroxibenzoico	3,92 ± 0,05	1,81 ± 0,49	0	Pizzeghello et al., 2006
	Ácido ferúlico	8,13 ± 0,52	6,43 ± 0,14	1,24 ± 0,02	Ferro et al., 2006
	Ácido 4-hidroxicinâmico	16,20 ± 0,82	6,56 ± 0,93	0,98 ± 0,08	*Ácido protocatecúico-similar:*
	Álcool sinapílico	0	1,21 ± 0,00	0	Pizzeghello et al., 2006
	Álcool coniferílico	0	0,91 ± 0,23	0	Singh et al., 2014

Classes de moléculas		LHC	SHC	DOM/SHC	Efeito AIA-similar
		μg g^{-1} (m/m)			
Alfa hidroxiácidos	Ácido glicérico	15,92 ± 1,10	12,54 ± 2,05	1,11 ± 0,08	
Alditóis	Glicerol	87,44 ± 6,37	85,26 ± 4,11	64,13 ± 9,19	
	Xilitol	19,27 ± 0,89	9,54 ± 1,74	0	
Monossacarídeos	6-Deoxi-D-glucose	8,27 ± 0,31	5,36 ± 0,59	3,67 ± 0,57	
	D (+)Altrose	4,23 ± 0,07	2,42 ± 0,36	0	
	D-Glucose	29,65 ± 1,65	19,55 ± 2,43	7,81 ± 0,22	
	D-Lixose	8,38 ± 0,33	33,56 ± 4,71	19,33 ± 1,57	
	D-Manose	25,52 ± 2,31	17,99 ± 2,50	2,61 ± 0,05	
	N-Acetil-D-manosamina	3,11 ± 0,87	2,10 ± 0,44	0	
	Talose	1,90 ± 0,02	4,05 ± 0,39	2,51 ± 0,17	
Nucleotídeos	Adenina	11,92 ± 0,72	9,25 ± 1,19	1,01 ± 0,07	
	Citosina	12,45 ± 0,47	4,32 ± 0,45	0	
	Timina	13,10 ± 1,00	8,43 ± 0,56	2,37 ± 0,11	

ANEXO

Anexo A – Comprovante de submissão do artigo.

De: **Science of the Total Environment** em@editorialmanager.com
Assunto: STOTEN-D-22-31455 - Confirming your submission to Science of the Total Environment
Data: 11 de dezembro de 2022 15:07
Para: Ramom Rachide Nunes ramom.rachide@ufrpe.br

Dear Professor Ramom Rachide Nunes,

Thank you for sending your manuscript A role for the auxin-like compounds in germination tests using corn waste hydrochar for consideration to Science of the Total Environment. It has been assigned the following manuscript number: STOTEN-D-22-31455. Please accept this message as confirmation of your submission.

When should I expect to receive the Editor's decision?
We publicly share the average editorial times for Science of the Total Environment to give you an indication of when you can expect to receive the Editor's decision. These can viewed here: http://journalinsights.elsevier.com/journals/0048-9697/review_speed

What happens next?
Here are the steps that you can expect as your manuscript progresses through the editorial process in the Editorial Manager (EM).

1. First, your manuscript will be assigned to an Editor and you will be sent a unique reference number that you can use to track it throughout the process. During this stage, the status in EM will be "With Editor".

2. If your manuscript matches the scope and satisfies the criteria of Science of the Total Environment, the Editor will identify and contact reviewers who are acknowledged experts in the field. Since peer-review is a voluntary service, it can take some time but please be assured that the Editor will regularly remind reviewers if they do not reply in a timely manner. During this stage, the status will appear as "Under Review".

Once the Editor has received the minimum number of expert reviews, the status will change to "Required Reviews Complete".

3. It is also possible that the Editor may decide that your manuscript does not meet the journal criteria or scope and that it should not be considered further. In this case, the Editor will immediately notify you that the manuscript has been rejected and may recommend a more suitable journal.

For a more detailed description of the editorial process, please see Paper Lifecycle from Submission to Publication:
http://help.elsevier.com/app/answers/detail/a_id/160/p/8045/

How can I track the progress of my submission?
You can track the status of your submission at any time at http://ees.elsevier.com/STOTEN

Once there, simply:
1. Enter your username: Your username is: [redacted]

If you need to retrieve password details, please go to: [redacted]

2. Click on [Author Login]. This will take you to the Author Main Menu
3. Click on [Submissions Being Processed]

Many thanks again for your interest in Science of the Total Environment.

Kind regards,
Science of the Total Environment

If you require further assistance, you are welcome to contact our Researcher Support team 24/7 by live chat and email or 24/5 by phone:
http://support.elsevier.com

This journal uses the Elsevier Article Transfer Service. This means that if an editor feels your manuscript is more suitable for an alternative journal, then you might be asked to consider transferring the manuscript to such a journal. The recommendation might be provided by a Journal Editor, a dedicated Scientific Managing Editor, a tool assisted recommendation, or a combination. For more details see the journal guide for authors.
#AU_STOTEN#

To ensure this email reaches the intended recipient, please do not delete the above code

Anexo B – Manuscrito submetido à revista *Science of the Total Environment.*

Science of the Total Environment

A role for the auxin-like compounds in germination tests using corn waste hydrochar

--Manuscript Draft--

Manuscript Number:	
Article Type:	Research Paper
Keywords:	Hydrothermal carbonization; Organic compounds; Hormone-like activity; Auxin-like property; Dissolved organic matter.
Corresponding Author:	Ramom Rachide Nunes, PhD Federal Rural University of Pernambuco Serra Talhada, Pernambuco BRAZIL
First Author:	Edson Thiago Gomes Lima, BSc
Order of Authors:	Edson Thiago Gomes Lima, BSc
	Érica Danúbia Souza Sales, BSc
	Rogerio Aquino Saraiva, PhD
	Ramom Rachide Nunes, PhD
Abstract:	This work studied the auxin-like activity of liquid and solid hydrochar from aboveground corn biomass prepared using hydrothermal carbonization (HTC). Bioassays were performed by testing liquid hydrochar concentrations in the range of 0.0557-5570.0 mg carbon L-1; and solid hydrochar in the range of 0.026-2600.0 mg carbon L-1. Dissolved organic matter (DOM) was extracted to perform tests using solid hydrochar. Bioassays were performed using seeds of Lactuca sativa. SEM, ATR-FTIR, and Py-GC/MS instrumental methods were used to assess the effect of HTC on hydrochar production/composition. Liquid hydrochar presented an intense bioactivity, completely inhibiting the germination of testing seeds at concentrations above 696 mg C L-1. Liquid hydrochar also was considerably more bioactive than the DOM, even though it has shown an auxin-like effect in the germination tests. SEM analysis showed how HTC transformed the feedstock surface by opening pores and grooves in the hydrochars. ATR-FTIR also showed that HTC changed the chemical composition of corn waste, reducing hydroxyl groups and enriching the material with aromatic functional groups. Py-GC/MS allowed the identification of the molecules involved in IAA-like effects: carboxylic acids (linear and aromatic) and amino acids. The concentration of more bioactive molecules, rather than their simple presence in the hydrochar fraction, determined the bio-stimulating effect, besides an excellent linear regression between auxin-like effect and the concentration of active molecules.
Suggested Reviewers:	Wander Gustavo Botero, PhD Professor, Federal University of Alagoas wander.botero@iqb.ufal.br
	Fulvia Tambone, PhD Professor, University of Milan fulvia.tambone@unimi.it
	Daniel Olk, PhD Researcher, US Department of Agriculture dan.olk@ars.usda.gov
	Deborah Pinheiro Dick, PhD Professor, Federal University of Rio Grande do Sul deborah.dick@ufrgs.br
	Eny Maria Vieira, PhD Professor, University of Sao Paulo eny@iqsc.usp.br
	Luciana Camargo Oliveira, PhD Professor, Federal University of Sao Carlos lcamargo@ufscar.br

	Leandro Antunes Mendes, PhD Researcher, Federal University of Mineiro Triangle leandro.mendes@uftm.edu.br
Opposed Reviewers:	

Dear Professors Damià Barceló, Jay Gan, Philip Hopke, and Elena Paoletti,
Co-Editors-in-Chief of Science of the Total Environment.

Please find attached the manuscript entitled A ROLE FOR THE AUXIN-LIKE COMPOUNDS IN GERMINATION TESTS USING CORN WASTE HYDROCHAR, authored by Edson T.G. Lima, Erica D.S. Sales, Rogerio A. Saraiva, and myself. We believe it should be published due to the following features:

i. This work fits the aims and scope of the Science of the Total Environment. It is an original and interdisciplinary environmental research paper focused on areas such as environmental technologies (hydrothermal carbonization, HTC), biology (germination tests and seed/plant development), chemistry (chemical composition and use of instrumental analysis applied in the hydrochar characterization and data acquisition of bioactive molecules), and agronomy (we recommend the hydrochar use in agriculture and plant production). Our paper describes laboratory trials and demonstrates noteworthy advances in methodology and understanding with a clear link to the environment (also agriculture);

ii. This work studied the use of aboveground corn biomass as feedstock in the production of hydrochars via hydrothermal carbonization (HTC). In addition, germination tests were performed, and organic compounds with hormonal activity (auxin-like effect) were assessed via Py-GC/MS. Other instrumental analyses were applied, such as ATR-FTIR and SEM;

iii. Bio-stimulant effects were assessed regarding solid and liquid fractions of hydrochar. Solid hydrochar was tested in terms of the extracted dissolved organic matter (DOM). Both fractions were bioactive; however, the liquid fraction was considerably more bio-stimulant in the germination tests. Using Py-GC/MS, the most active molecular classes were determined, and the reasons for the difference in the auxin-like effect were elucidated (see next point);

iv. Finally, the most crucial finding of this study concerns how the HTC produces or concentrates organic molecules able to bio-stimulate vegetal production on germination tests. Among the molecular classes determined, amino acids and carboxylic acids (linear and aromatic) are suggested as responsible for the intense auxin-like effect in liquid hydrochar. In the next step of this study, HTC will be scaled up, and the real use of hydrochars will be evaluated, first in pot cultivation, followed by field application.

Thank you for your time and consideration.

Sincerely,

Prof. Ramom Rachide Nunes
Laboratory of Environmental Chemistry
Federal Rural University of Pernambuco, Brazil

Graphical abstract

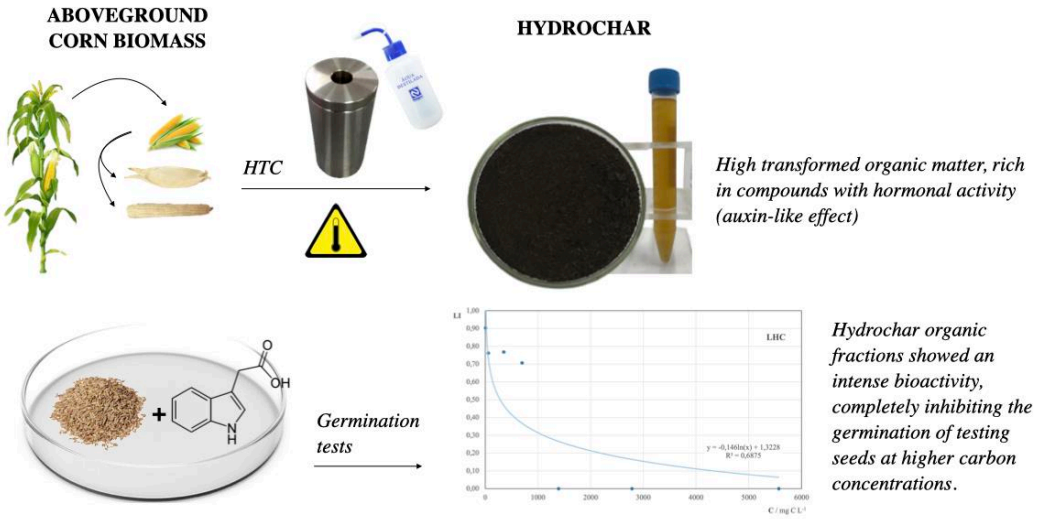

Highlights

- Hydrotermal carbonization converts corn waste into hydrochar.
- Hydrochar can have biostimulating effect for the presence of hormone-like compounds.
- Auxine-like activity was more intense in liquid than solid hydrochar (DOM).
- Amino acids and carboxylic acids were reported to act as IAA-like molecules.

A ROLE FOR THE AUXIN-LIKE COMPOUNDS IN GERMINATION TESTS USING CORN WASTE HYDROCHAR

EDSON THIAGO GOMES LIMA[1]; ÉRICA DANÚBIA SOUZA SALES[2]; ROGÉRIO DE AQUINO SARAIVA[3] and RAMOM RACHIDE NUNES[1*].

[1] *Laboratory of Environmental Chemistry, Federal Rural University of Pernambuco, Serra Talhada, Brazil.*

[2] *Academic Unit of Serra Talhada, Federal Rural University of Pernambuco, Serra Talhada, Brazil.*

[3] *Teacher Training Institute, Federal University of Cariri, Brejo Santo, Brazil.*

ORCID: EDSON THIAGO GOMES LIMA: 0000-0001-8005-7493

ÉRICA DANÚBIA SOUZA SALES: 0000-0002-4554-0460

ROGÉRIO AQUINO SARAIVA: 0000-0001-5812-5525

RAMOM RACHIDE NUNES: 0000-0001-9290-4354

* Address correspondence to Ramom Rachide Nunes, Federal Rural University of Pernambuco, Serra Talhada, Pernambuco, Brazil; Phone: +55 87 3929-3089

E-mail: ramom.rachide@ufrpe.br

Abstract

This work studied the auxin-like activity of liquid and solid hydrochar from aboveground corn biomass prepared using hydrothermal carbonization (HTC). Bioassays were performed by testing liquid hydrochar concentrations in the range of 0.0557-5570.0 mg carbon L^{-1}; and solid hydrochar in the range of 0.026-2600.0 mg carbon L^{-1}. Dissolved organic matter (DOM) was extracted to perform tests using solid hydrochar. Bioassays were performed using seeds of *Lactuca sativa*. SEM, ATR-FTIR, and Py-GC/MS instrumental methods were used to assess the effect of HTC on hydrochar production/composition. Liquid hydrochar presented an intense bioactivity, completely inhibiting the germination of testing seeds at concentrations above 696 mg C L^{-1}. Liquid hydrochar also was considerably more bioactive than the DOM, even though it has shown an auxin-like effect in the germination tests. SEM analysis showed how HTC transformed the feedstock surface by opening pores and grooves in the hydrochars. ATR-FTIR also showed that HTC changed the chemical composition of corn waste, reducing hydroxyl groups and enriching the material with aromatic functional groups. Py-GC/MS allowed the identification of the molecules involved in IAA-like effects: carboxylic acids (linear and aromatic) and amino acids. The concentration of more bioactive molecules, rather than their simple presence in the hydrochar fraction, determined the bio-stimulating effect, besides an excellent linear regression between auxin-like effect and the concentration of active molecules.

Keywords: Hydrothermal carbonization, Organic compounds, Hormone-like activity, Auxin-like property, Dissolved organic matter.

1 Introduction

Corn (*Zea mays*) is one of the most important crops in the world, with a global production of 1.168 billion metric tons in the harvest of 2022/2023 (USDA, 2022). However, intensive corn culture usually generates a great deal of agricultural waste, which can harm the environment when improperly disposed of. In order to avoid pollution, specific chemical, physical and biological treatments have been adopted to reduce waste amount, enhancing waste corn use/recycling systems (Awogbemi and Kallon, 2022).

In this perspective, hydrothermal carbonization (HTC) is reported to be an effective treatment for agricultural waste, adding value by improving the organic matter (OM) quality and nutrient availability. HTC is generally performed using water as a reaction medium, moderate temperatures (180-250ºC), and self-generated pressure. As a product, HTC converts the moist feedstock into a carbonaceous material named hydrochar. In addition, HTC also generates a liquid fraction derived from the fusion/ dissolution of the more labile organic molecules in the solution. HTC also is considered an economic and ecological method due to the low applied energy and the small generation of unwanted by-products, such as CO_2 (Ayodele et al., 2022; Chen et al., 2021; Lang et al., 2022). During the HTC, water in a subcritical state generally promotes transformations in the OM feedstock. First, the OM suffers hydrolysis, attended by dehydration and decarboxylation. Furthermore, carbon chains are condensed and aromatized, providing material of higher elemental carbon than feedstock (Haris et al., 2022; Lin et al., 2022; Mariuzza et al., 2022).

Finally, hydrochar presents low atomic ratios of O/C and H/C, indicating OM stability. In addition, hydrochar also offers a high concentration of functional groups and a high surface area, which positively influence the cation-exchange capacity (CEC), besides the

nutrient retention and availability (Bento et al., 2021; Khosravi et al., 2022; Mohammadi et al., 2022; Zhang et al., 2021).

Depending on the hydrochar characteristics, different forms of use can be intended, e.g., as agricultural input (Hou et al., 2020; Kavindi et al., 2022), adsorbent material (Ighalo et al., 2022; Lang et al., 2021), solid fuel (Kang et al., 2019; Mariuzza et al., 2022), as catalyst (Quevedo-Amador et al., 2022; Shuang et al., 2022) etc. Among these applications, hydrochar use in agriculture is the most common, mainly applied in environmental remediation as a soil conditioner; and in modern systems of agriculture, supplying OM and nutrients to the soil, aiming to promote plant nutrition and vegetal production (Bento et al., 2021; Khosravi et al., 2022).

Many studies have reported the potential use of hydrochars in agriculture. Bento et al. (2019) assessed the release of nutrients and OM of vinasse hydrochar in different soils, concluding that hydrochar was an efficient organic fertilizer with the potential to improve agricultural productivity. Hou et al. (2020) showed how the application of sawdust hydrochar in rice cultivation increased productivity and significantly reduced the emission of greenhouse gases. Kavindi et al. (2022) produced hydrochars from rice straw and sewage sludge, showing their efficiency in remediating soil contaminated by Cr(VI).

Several studies have indicated that part of the role of OM in promoting plant development is associated with the presence of vegetal hormones, especially those from the auxin group. On the other hand, some authors have reported the presence of organic molecules, different from auxin but similar in hormonal effect/action. In this case, molecules with this effect are named compounds with hormone-like activity (Castillo-Esparza et al., 2021; Nardi et al., 2002; Scaglia et al., 2015).

Auxin-like activity is the influence of organic molecules from the OM on the vegetal metabolism, similar to the effect of auxin in fact, regulating, e.g., root growth, nutrient absorption, and consequently the vegetal production (Nardi et al., 2002; Scaglia et al., 2015)

In recent studies, Wang et al. (2022) evaluated the phytotoxicity of cabbage hydrochar via germination tests, obtaining favorable results for root growth. Sun et al. (2022) produced hydrochar from reed straw. They evaluated its influence on the growth of peanut seedlings in saline soil, reporting an increase in the content of plant hormones in the vegetal tissues. Bento et al. (2021) evaluated the bio-stimulant potential of vinasse hydrochar on corn seed germination, indicating the presence of phytotoxic compounds that inhibited seed germination.

Amino acids and organic carboxylic acids (oxalic, tartaric, and phenolic acids) were reported to present auxin-like effects when tested as pure molecules or present as constituents of the organic fraction (i.e., dissolved organic matter or some humic substance fraction) (Colla et al., 2014; Pizzeghello et al., 2006; Singh et al., 2014).

The chemical complexity of OM renders difficult the analytical identification of auxin-like molecules promoting the bio-stimulation effect, and this has led to attempts to identify which of the organic fractions composing OM have auxin-like properties (Canellas et al., 2002; Dell'Agnola and Nardi, 1987; Quaggiotti, 2004). For example, humic acids fractionation into low molecular (HALMW) and high molecular weight (HAHMW), and water-soluble fractions (WHA) (Zandonadi et al., 2013), indicated that molecular weight did not affect the auxin-like activity (Dell'Agnola and Nardi, 1987; Muscolo, 1999). A possible explanation of this result is that hormone-plant receptors

115 interact with small auxin-like molecules present in OM rather than the total OM (Canellas
116 et al., 2011; Trevisan et al., 2010; Zandonadi et al., 2013).

117 This work aimed to study the auxin-like effect of hydrochar prepared from corn waste via
118 the hydrothermal carbonization process (HTC). In particular, using different analytical
119 approaches, i.e., ATR-FTIR and Py-GC/MS, organic molecules responsible for bio-
120 stimulant effects were investigated.

121

122 **2 Materials and Methods**

123 *2.1 Hydrochar production*

124 This study was carried out using hydrochar prepared from corn waste.

125 Hydrothermal carbonizations (HTC) were set up in a Teflon reactor coated with titanium
126 and a volume of 100 mL. Hydrochars were prepared using 1 g of corn waste and 50 mL
127 of water. The reactor was maintained at 200ºC in a stove (Sterilifer SX, São Caetano do
128 Sul, Brazil) for 12 h. These conditions were previously defined through a preliminary 2^3
129 factorial design.

130 Corn waste was collected in a settlement of the Landless Workers' Movement (MST),
131 located in the municipality of Serra Talhada, Pernambuco, Brazil (9°16'15.8"S
132 40°35'32.6"W). Corn waste was collected from aboveground biomass in forms of stem,
133 leaves, straw, and corn cob. Fresh feedstocks were mixed (based on dry volume), and the
134 proportion was determined by combining each residue in the harvested plant: 81% stem
135 and leaves, 10% straw, and 9% corn cob. The mixture was crushed in a knife mill and
136 sieved between 500 and 250 mm. The following analyses were carried out aiming to
137 characterize the mixed feedstock: organic matter (OM) (NEN, 1994), total organic carbon

138 (TOC) (using Sievers InnovOX GE carbon analyzer, Boulder, USA), and O/C and H/C
139 ratios (through elemental analysis, using a Perkin Elmer Series II CHNS/O Analyser
140 2400, Waltham, USA).

141 After HTC, a suspension was obtained and separated by filtration. The liquid fraction
142 (sample LHC) was stored at -4 ºC, and the solid fraction (sample SHC) was dried in a
143 stove at 60 ºC for 24 h and then stored in a desiccator. Germination tests were carried out
144 in the liquid fraction of the hydrochar (LHC) and the dissolved organic matter (DOM)
145 extracted from the solid fraction (SHC). The experiments were carried out at the
146 Laboratory of Environmental Chemistry (LEC), Federal Rural University of Pernambuco
147 (UFRPE), Brazil.

148

149 *2.2 Dissolved organic matter (DOM) extraction*

150 DOM was extracted using 5 g of hydrochar in a 250 mL Erlenmeyer and 100 mL distilled
151 water. The sample was heated in a Dubnoff bath at 40°C with stirring at 60 rpm for 30
152 min. Then, the supernatant was filtered in a pressurized system using cellulose acetate
153 filters of 0.45 μm (Whatman) and stored in a refrigerator at -4 °C (D'Imporzano and
154 Adani, 2007).

155

156 *2.3 Hydrochar characterization*

157 Liquid (LHC) and solid (SLH) hydrochar were characterized in terms of total organic
158 carbon (TOC) (using a Sievers InnovOX carbon analyzer, VEOLIA, Aubervilliers,
159 France), ratios O/C and H/C (via elemental analysis, using a Perkin Elmer Series II
160 CHNS/O Analyser 2400, Waltham, USA), pH (using a pH meter Tecnal, Piracicaba,

161 Brazil), and electrical conductivity (EC) (using a conductivity meter model Tecnal Tec-
162 4MP, Piracicaba, Brazil). Furthermore, in solid hydrochar (SHC), the organic matter
163 (OM) (NEN, 1994) was also determined.
164

165 *2.4 SEM analysis*

166 Hydrochar (SHC) and corn waste were analyzed and compared by Scanning Electron
167 Microscopy (SEM). Samples were mounted on aluminum stubs and covered with gold
168 using a metalized DENTON VACUUM model DESKV (Moorestown, USA).
169 Micrographs were obtained in a scanning electron microscope TESCAN VEGA3
170 (Libušina, Czechia).
171

172 *2.5 ATR-FTIR analysis*

173 Spectra in the infrared region were obtained from a spectrophotometer Shimadzu IR-
174 Tracer 100 (Kyoto, Japan) and sampling of Attenuated Total Reflectance (ATR) of
175 diamond/zinc selenide and crystal performance, with a resolution of 4 cm^{-1} and 16
176 accumulations. The analyzed region ranged between 4000-600 cm^{-1}.
177

178 *2.6 Py-GC/MS characterization*

179 Chromatographic analysis was performed on an Agilent 5975C Series GC/MS (Santa
180 Clara, USA) and a capillary column of 30.00 m × 250.00 μm × 0.25 μm ZB-Semivolatiles.
181 He was used as the carrier gas, injected at a flow rate of 1.1 mL min^{-1}. A volume of 1.0
182 μL of the sample was injected using a pyrolyzer injector (CDS 4000, Oxford, USA) in
183 splitless mode. The temperature program was set at 60°C for 1 min and then increased to

184 325°C at a rate of 10°C min^{-1}. Mass spectra were obtained by electronic impact at 70 eV,
185 and data was collected between 50-660 m/Z. The compounds were identified by
186 comparison with mass spectra from the Agilent Fiehn GC/MS Metabolomics RTL
187 Library, using AMDIS software (Automated Mass Spectral Deconvolution and
188 Identification System software, NIST 08).

189 Regarding the LHC, the sample was first lyophilized to eliminate water and thus
190 concentrate the OM. A lyophilizer LabConco Benchtop (Kansas, USA) was used in
191 standard mode for 48 h.

192

193 *2.7 Hormone-like activity tests using bioassays*

194 The auxin-like activities of the HAs were assessed by checking the root growth inhibition
195 of lettuce seeds (*Lactuca sativa*, ISLA, Porto Alegre, Brazil). Bioassays were prepared
196 by placing 30 seeds in Petri dishes containing a filter paper (Whatman 91) wetted with
197 3.0 mL of distilled water (control) or 3.0 mL of the sample solution in the following
198 concentrations:

199 LHC: 0.0557; 0.557; 5.57; 55.7; 348.125; 696.25; 1392.5; 2785.0 and 5570.0 mg C L^{-1}.

200 SHC: 0.026; 0.26; 2.6; 26.0; 162.5; 325.0; 650.0; 1300.0 and 2600.0 mg C L^{-1};

201 To obtain the calibration curve, tests were performed using 0.2, 0.1, 0.06, 0.04, 0.01,
202 0.006, 0.004, and 0.001 mg C L^{-1} of auxin (3-indoleacetic acid, IAA, Sigma Aldrich,
203 I3750). The seeds were germinated in dark conditions at 25 °C; after 5 days, the seedlings
204 were removed and the root lengths measured (Pizzeghello et al., 2006).

205 Root length was defined from the tip of the root to the point where the radicle emerged
206 from the seed coat. Root lengths below 5 mm were considered non-germinated seeds
207 (Pizzeghello et al., 2006; Wang et al., 2001).

208 Data were presented as a length index (LI), calculated by dividing the mean length of the
209 sample and the mean of the length obtained in control.

210 The hormone-like activity was considered present when LI vs. [C] trend was statistically
211 significant (Sig. < 0.05) and followed a logarithmic curve (Ertani et al., 2013; Pizzeghello
212 et al., 2006).

213

214 *2.8 Statistical analysis*

215 One-way bootstrap ANOVA was used to evaluate the differences between the means for
216 $p < 0.01$, using Duncan's multiple range tests. Linear bootstrap regression was applied to
217 determine the relationship of hormone-like effect vs. bio-stimulant molecules dose. IBM
218 SPSS Statistics v. 29 was used for data analysis.

219

220 **3 Results and Discussion**

221 *3.1 Hydrochar production*

222 The chemical characteristics of hydrochars are shown in Table 1. From observing these
223 parameters, we can follow the effect of hydrothermal carbonization on OM evolution,
224 i.e., changes in color and particle size (texture), in addition to a significant TOC increase
225 and a slight OM decrease (Table 1).

Table 1. Chemical characterization of corn waste and liquid/solid hydrochars.

	Corn waste[c]	SHC[c]	SHC/DOM[ac]	LHC
OM[a] (%)	97.19 ± 0.11b	91.35 ± 0.26a	-	-
TOC[ab]	43.32 ± 0.00a	73.13 ± 0.00b	2.60 ± 0.00	5.57 ± 0.00
pH	-	-	4.55 ± 0.01b	3.71 ± 0.00a
EC (μS cm^{-1})	-	-	2.90 ± 0.03a	3.84 ± 0.00b
Elemental analysis				
H (%)	7.79 ± 0.01c	5.85 ± 0.02bc	5.52 ± 0.02b	4.19 ± 0.02a
N (%)	3.12 ± 0.00b	3.39 ± 0.01b	2.02 ± 0.02a	2.99 ± 0.02a
O (%)	35.08 ± 0.04c	15.35 ± 0.03a	16.32 ± 0.02ab	20.85 ± 0.08b
Molar ratio				
O/C[d]	0.81 ± 0.01b	0.21 ± 0.01a	-	-
H/C[d]	0.18 ± 0.00b	0.08 ± 0.00a	-	-

[a] OM = Particulate organic matter; TOC = Total organic carbon; EC = Electrical conductivity; SHC/DOM = Dissolved organic matter extracted from the solid hydrochar.

[b] TOC units: Corn waste and SHC in %; LHC and SHC/DOM in g L^{-1}. Values of TOC were used to calculate O/C and H/C ratios.

[c] Values in the same row followed by the same letter are not statistically different at $p < 0.05$, according to ANOVA One-way and Duncan's test.

[d] O/C and H/C standard deviation was calculated as: $std = O/C \times [(std\ O \div O)^2 + (std\ C \div C)^2]^{1/2}$ and $std = H/C \times [(std\ H \div H)^2 + (std\ C \div C)^2]^{1/2}$.

Solid hydrochar presented a black color, different from the yellowish tone showed by corn waste, indicating OM carbonization. Smaller particle sizes were obtained in powder form in the hydrochar, different when compared to the fresh waste (500-250 mm). Changes in color and particle size are evidence of the high degree of biomass carbonization (Santana et al., 2022). Based on preliminary tests, longer HTC (over 10 h) and higher temperatures (maximum 200°C allowed by Teflon) favored the process. In this case, the mean HTC yield was 57.35% (m/m). The melting of organic molecules and the solubilization of some compounds in water contributed to decreasing the hydrochar yield (sample SHC) (Farobie et al., 2022; Venkatesan et al., 2022; Zhang et al., 2019). On the other hand, molten chains enriched the liquid fraction with organic compounds, as observed. The mean yield of liquid fraction (LHC) was 27%. Only HTC above 180° originated the liquid fraction.

TOC increased 52% in the SHC when compared to corn waste. OM decreased by 6.4%. Changes in the carbon content are mainly related to (macro)molecule breaks, dehydration processes, decarboxylation, and the subsequent condensation and aromatization of the carbon chains, concentrating the organic carbon in the hydrochar (Li and Cai, 2022; Wang et al., 2020).

Significant decreases in both the H/C ratio and O/C indicated the high degree of OM transformation during the HTC process. The H/C ratio reduced from 0.18 in the feedstock to 0.08 in the hydrochar (76% of difference). O/C passed from 0.81 to 0.21 (117% of difference). Both ratios are statistically different according to ANOVA One-way and Duncan's test at $p < 0.05$.

The molar H/C ratio is an important parameter to determine the hydrochar quality. In general, the H/C ratio change substantially when a thermochemical treatment is efficient,

and values below 0.7 are recommended. In addition, O/C ratio is correlated with the hydrochar stability. The H/C ratio is a property correlated with the degree of thermochemical alteration that produces fused aromatic ring structures in the hydrochar. The presence of these structures is an intrinsic measure of molecular stability (Calvelo Pereira et al., 2011; Sevilla and Fuertes, 2009; Spokas, 2010). Results agreed with the literature that reported low H/C and O/C rations after the HTC process (Aragón-Briceño et al., 2020; Santana et al., 2022; Sevilla and Fuertes, 2009).

3.2 SEM analysis

SEM micrographs are shown in Figure 1. Three micrographs are presented in the scales of 10, 50, and 100 μm, comparing the surfaces of corn biomass and sample SHC. Microscopy images indicated how the hydrothermal carbonization acted on the feedstock, changing the material by opening pores and grooves.

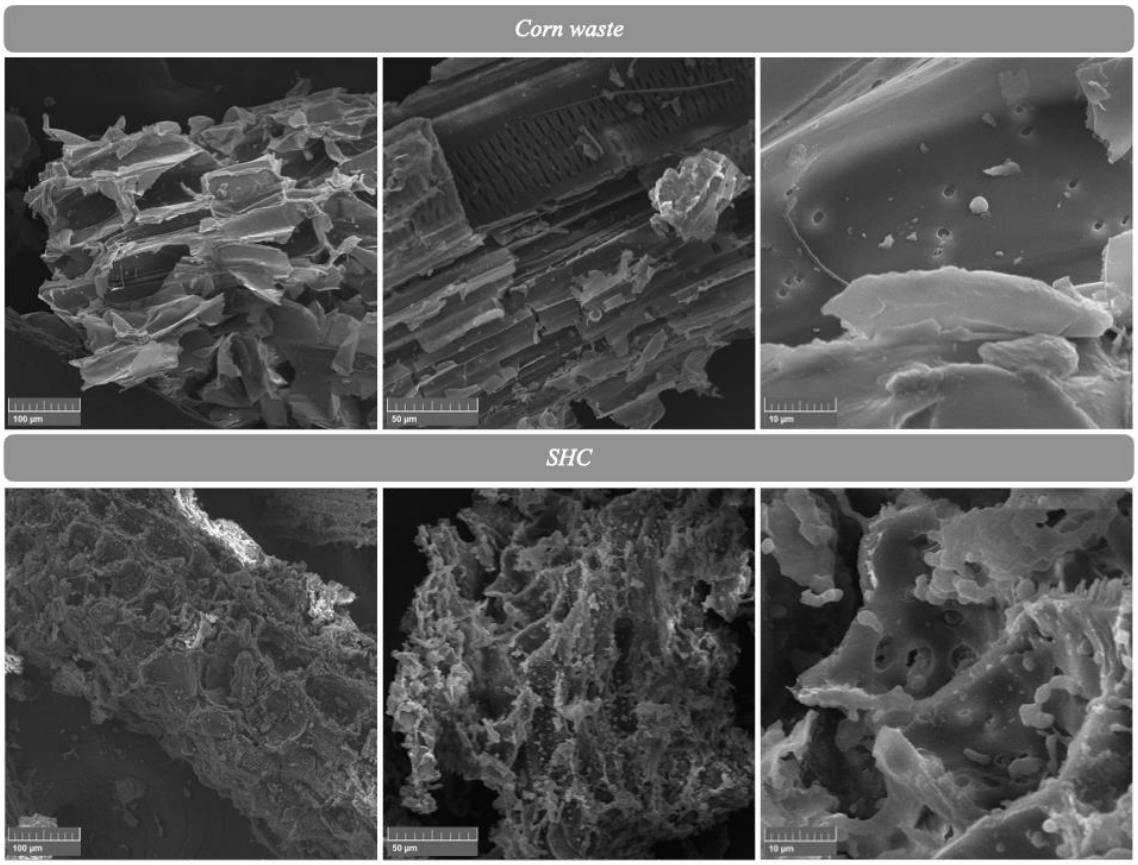

Figure 1. Corn waste and SHC surface morphology by SEM.

SEM identified no pores with nano-dimension at a magnification of 1,000X. However, the presence of structured pores was confirmed, thus increasing the hydrochar surface area and consequently favoring the retention of ions, moisture, and organic compounds.

HTC also promoted a rough feature on the hydrochar surface compared to corn waste. This surface change was more evident in the scales of 100 and 50 μm. In addition, the distribution of cavities is apparently homogeneous along the hydrochar structure. This aspect is essential for promoting greater surface area and adsorption capacity.

3.3 ATR-FTIR analysis

Spectra of ATR-FTIR are shown in Figure 2. In general, each spectrum is significantly different and indicates how molecular/functional groups were changed during the HTC when corn waste was converted into hydrochar (SHC and LHC).

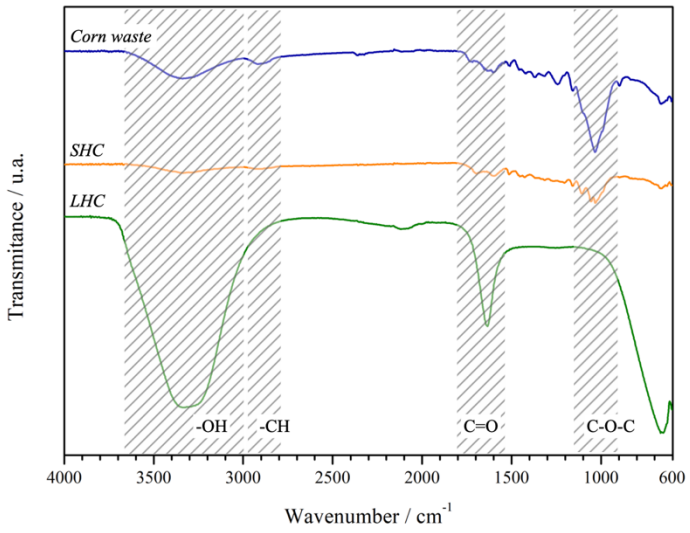

Figure 2. ATR-FTIR spectra of corn waste and hydrochars (LHC and SHC)

The band at 3300 cm^{-1} in the corn waste, attributed mainly to -OH stretching vibrations present in water and polysaccharides, has a low intensity in the SHC, indicating the feedstock dehydration due to the temperature increase in the HTC, in addition to the breakdown of polysaccharide molecules. In LHC, water from the hydrochar aqueous phase intensified this band, indicating the presence of dissolved hydroxyl groups and phenolic compounds (Santana et al., 2022).

The region between 3000 and 2800 cm^{-1} in the corn waste is associated with $–CH_3$, $–CH_2$, and –CH bonds and decreased after HTC in sample SHC (Farobie et al., 2022; Santana et al., 2022).

297 In the region between 1700 and 1400 cm^{-1}, bands observed in the corn waste are
298 associated with functional groups containing C=O. These bands are of smaller intensity
299 in SHC, indicating that decarboxylation reactions have occurred during the HTC process
300 (Farobie et al., 2022; Santana et al., 2022; Wang et al., 2020).

301 The band at 1600 cm^{-1} in LHC is attributed to the elongation of C=C and C–H bonds in
302 aromatic compounds, while the band at 690 cm^{-1} is associated mainly with angular
303 deformations of aromatic rings, indicating the strong aromatic nature of the liquid fraction
304 (Liu et al., 2021; Zhang et al., 2019).

305 The band present in the corn waste at 1000 cm^{-1} is associated with the stretching of C–O
306 and C–O–C bonds in polysaccharides, such as cellulose. In SHC, this intensity has
307 decreased, indicating cellulose degradation by the high temperature and pressure during
308 the HTC (Farobie et al., 2022; Santana et al., 2022; Wang et al., 2020).

309

310 *3.4 Hormone-like activity test*

311 Solid and liquid hydrochar were tested for auxin-like properties (IAA-like effect). Solid
312 hydrochar was tested in terms of the extracted DOM. The results of bioassays indicated
313 that both forms had hormone–like activity (Tables 2, 3). LHC inhibited the growth of all
314 roots at the highest concentrations, above 696.25 mg C L^{-1}. However, SHC partially
315 inhibited at all concentrations, even at the highest concentration, without completely
316 inhibiting root growth. This result was expected since the carbon difference was
317 significant between the samples (Table 1). Results agreed with the literature that reported
318 IAA-like activity for hydrochars (Bento et al., 2020; Egamberdieva et al., 2020; Massaya
319 et al., 2022; Sun et al., 2022).

320 The bioassays tests were performed on a wide carbon concentration range
321 (0.026 – 2600 mg C L^{-1} to SHC and 0.0557 – 5570 mg C L^{-1} to LHC). However, IAA-
322 like activity was verified for SHC in the concentration range 26 – 2600 mg C L^{-1} and
323 5.57 – 5570 mg C L^{-1} to LHC. In other words, IAA-like activity was verified from 1%
324 and 0.1% of the total C concentration, respectively. The angular coefficient of logarithmic
325 curves (LI/[C]) was used to evaluate IAA-like activity intensity (Scaglia et al., 2015),
326 obtaining the following scale: SHC < LHC (Table 3). The most effective IAA-like effect
327 was found for LHC, suggesting that the fusion of more labile molecules enhanced the
328 development of IAA-activity due to the transformation that occurred during the HTC
329 process.

330 **Table 2.** Length index (LI) of *Lactuca sativa* roots after applying liquid and solid hydrochars and 3-indoleacetic acid (IAA).

SHC		LHC		IAA	
DOM doses (mg C L^{-1})	LI[a] (length index)	Doses (mg C L^{-1})	LI[a]	Doses (mg C L^{-1})	LI[a]
26	0.91 ± 0.06abc [a]	5.57	0.90 ± 0.03bc	0.001	0.49 ± 0.22d
162.5	0.85 ± 0.07abc	55.7	0.76 ± 0.06bc	0.004	0.28 ± 0.06c
325	0.85 ± 0.08abc	348.125	0.77 ± 0.07bc	0.006	0.11 ± 0.02b
650	0.67 ± 0.60abc	696.25	0.71 ± 0.05b	0.01	0.06 ± 0.01a
1300	0.67 ± 0.01ab	1392.5	0.00 ± 0.00a	0.04	0.04 ± 0.01a
2600	0.62 ± 0.06a	2785	0.00 ± 0.00a	0.06	0.04 ± 0.04a
-	-	5570	0.00 ± 0.00a	0.1	0.02 ± 0.02a

331 [a] Values in the same column followed by the same letter are not statistically different at $p < 0.05$ from each other, according to ANOVA One-way

332 and Duncan's test.

333 **Table 3.** Hormone-like activity (IAA-like effect) observed in bioassays with liquid and solid hydrochar and 3-indoleacetic acid (IAA).

	Interval of IAA-like activity (mg C L− 1)	IAA-like effect equation	R^2	Sig.
SHC[a]	26.0-2600.0 mg C L^{-1}	$y = -0.068 \times ln(x) + 1.168$	0.856	0.022
LHC	5.57-5570.0 mg C L^{-1}	$y = -0.146 \times ln(x) + 1.323$	0.687	0.001
AIA	0.001-0.01 mg C L^{-1}	$y = -0.193 \times ln(x) - 0.834$	0.962	0.019

334 [a] Solid hydrochar was tested in the form of the extracted dissolved organic matter (DOM).

335 *3.5 Py-GC/MS characterization*

336 The results discussed above indicated the presence of hormone-like activity in solid and
337 liquid hydrochar.

338 The Py-GC/MS approach supported important information about the presence and
339 amount of specific molecules contained in the SHC and LHC. Now it can be used to
340 elucidate which molecules were responsible for the bio-stimulant effect.

341 DOM extracted from SHC and LHC were characterized by different classes of molecules
342 such as monosaccharides, amino acids, nucleotides, linear and aromatic carboxylic acids,
343 alpha hydroxyl acids, and alditoles (Table S1).

344 In general, LHC and SHC presented approximately the same concentration of organic
345 compounds, divided into molecular classes, totalizing 358.01 ± 12.33 μg g^{-1} in LHC and
346 300.26 ± 11.91 μg g^{-1} in SHC. Statistical differences were observed only in the following
347 classes: nucleotides, alditoles, aromatic carboxylic acids, and amino acids (ANOVA
348 bootstrap, $p < 0.05$); however, no difference between molecular classes exceeded 18%.
349 On the other hand, the DOM extracted from the SHC presented a total of
350 124.84 ± 21.91 μg g^{-1} of organic compounds, a sum considerably below the results of
351 LHC and SHC, also statistically different in all molecular classes (ANOVA bootstrap,
352 $p < 0.05$) (Fig. 3).

353

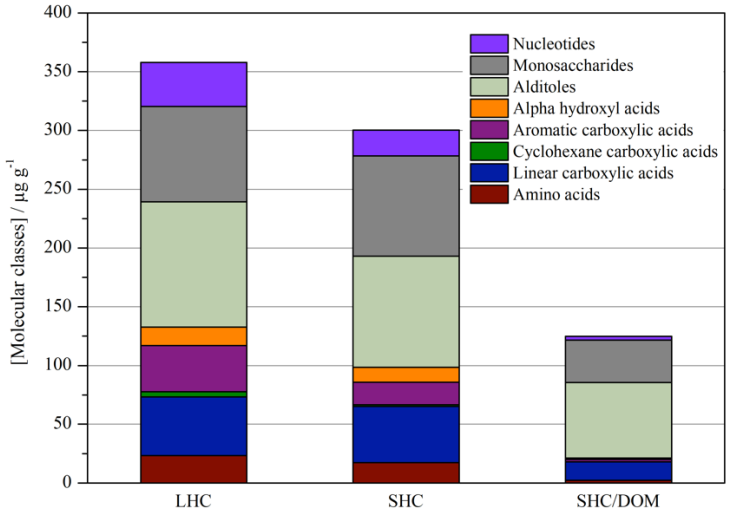

354

355 *Figure 3. Organic molecules detected in hydrochars and DOM by Py-GC/MS.*

356

357 Table S1 and Figure 3 indicate why even though both samples have auxin-like activity
358 (Table 3), the effects observed in the germination tests with LCH and SHC/DOM are so
359 different. Compounds such as alpha hydroxyl acids, aromatic carboxylic acids,
360 nucleotides, and amino acids were quantified between 0 and 3.38 ± 0.11 µg g^{-1} in
361 SHC/DOM.

362 In particular, carboxylic acids (both aromatics and linear) and amino acids have been
363 reported by many studies to have AA-like effects (Colla et al., 2014; Ertani et al., 2009;
364 Pizzeghello et al., 2006; Singh et al., 2014; Trevisan et al., 2010). A high presence of
365 carboxylic groups was correlated to the auxin effect (Trevisan et al., 2010). In addition,
366 amino acids have been reported by strong or weak IAA-like effects (Colla et al., 2014;
367 Ertani et al., 2009) depending on the presence of tryptophan (the IAA metabolic
368 precursor) or, more generally, by the amino acids' concentration (Colla et al., 2014; Ertani
369 et al., 2009). Moreover, the IAA-like effectiveness also was directly associated with the
370 concentration of specific aromatic carboxylic acids (i.e., vanillin, ferulic acid,

371 protocatechuic acid, 4-hydroxybenzoic acid, and 4-hydroxycinnamic acid)(Ferro et al.,
372 2006; Pizzeghello et al., 2006; Singh et al., 2014).

373 However, the complex chemical composition reported in Table S1 did not allow us to
374 clearly explain the bio-stimulating effect of SHC and LHC, as bio-stimulating molecules
375 were present in the samples studied. Nevertheless, many authors have reported that only
376 the presence of specific molecules is insufficient to get stimulating effects since molecular
377 concentration and bioavailability also play essential roles (Colla et al., 2014; Dobbss et
378 al., 2010; Pizzeghello et al., 2006). Now, taking into consideration the total concentration
379 in LHC and SHC/DOM (samples applied in the germination tests) of molecules
380 presenting IAA-like activity, each class had its concentration sum, i.e., carboxylic acids
381 and amino acids (Table S1), and the effect compared between samples, associating the
382 most reported group of molecular classes that presents IAA-like effect (Fig. 4). In LHC,
383 the sum of active molecules concentration was 112.36 ± 3.58 µg g^{-1} (concentration range
384 between 23.26 ± 4.81 µg g^{-1} and 50.14 ± 3.62 µg g^{-1}) and in SHC active molecules
385 concentration was 20.29 ± 2.92 µg g^{-1} (concentration range between 2.22 ± 0.69 µg g^{-1}
386 and 15.85 ± 0.42 µg g^{-1}).

387

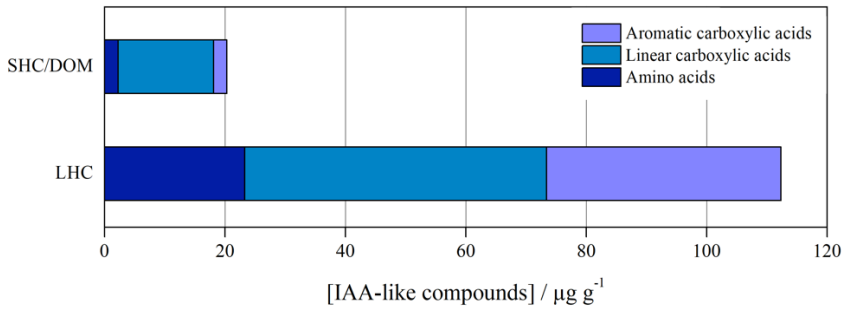

388

389 *Figure 3. IAA-like compounds in LHC and SHC/DOM determined by Py-GC/MS.*

390

391 SHC/DOM and LHC were statistically different (ANOVA bootstrap, $p < 0.05$),
392 suggesting that a higher concentration of bio-stimulating molecules resulted in an
393 effective bio-stimulant activity. Results indicated that even presenting a low
394 concentration of IAA-like compounds and much lower bioactivity, a bio-stimulating
395 effect was observed in sample SHC/DOM, as reported in Table 2. Thus, solid hydrochar
396 can be considered bioactive and positively influence plant development, as demonstrated
397 in the germination tests. This hypothesis was corroborated by the significant linear
398 regression between the IAA-like coefficient (Table 3). Anyhow, taking into consideration
399 how above discussed and the data reported in Fig. 3, it can be concluded that a bio-
400 stimulant molecules concentration of 20 $\mu g\ g^{-1}$ could be indicated as the limit above which
401 a more intense bio-stimulant effect started, even considering the effect caused by the
402 presence IAA-like compounds in small concentration.

403

404 **4 Conclusion**

405 Hydrochar prepared from aboveground corn biomass was tested for hormone-like activity
406 (auxin effect). Our findings indicated that hydrothermal carbonization affected this
407 activity by concentrating and producing carboxylic acid (aromatic and linear) and amino
408 acids, all of these molecules suggested as responsible for the hormone-like activity.
409 Liquid hydrochar was considerably more bioactive than the dissolved organic matter
410 extracted from the solid hydrochar, even presenting an auxin-like effect in the
411 germination tests. A total molecules concentration of 20 $\mu g\ g^{-1}$ was shown as a threshold
412 molecule concentration above which produced a more intense bio-stimulant activity.

413

414 **Acknowledgments**

The authors would like to thank FACEPE - *Fundação de Amparo à Ciência e Tecnologia do Estado de Pernambuco* (Recife, Brazil) for providing grants to E. T. G. Lima (Process Number BIC-0821-1.06/22).

References

Aragón-Briceño, C.I., Grasham, O., Ross, A.B., Dupont, V., Camargo-Valero, M.A., 2020. Hydrothermal carbonization of sewage digestate at wastewater treatment works: Influence of solid loading on characteristics of hydrochar, process water and plant energetics. Renew Energy 157, 959–973. https://doi.org/10.1016/J.RENENE.2020.05.021

Awogbemi, O., Kallon, D.V. von, 2022. Valorization of agricultural wastes for biofuel applications. Heliyon 8, e11117. https://doi.org/10.1016/j.heliyon.2022.e11117

Ayodele, O.O., Adekunle, A.E., Alagbe, O.A., Anguruwa, G.T., Ademola, A.A., Odega, C.A., Dornack, C., 2022. Application of biomass-derived hydrochar in process stability of anaerobic digestion. Bioresour Technol Rep 17, 100903. https://doi.org/10.1016/j.biteb.2021.100903

Bento, L.R., Castro, A.J.R., Moreira, A.B., Ferreira, O.P., Bisinoti, M.C., Melo, C.A., 2019. Release of nutrients and organic carbon in different soil types from hydrochar obtained using sugarcane bagasse and vinasse. Geoderma 334, 24–32. https://doi.org/10.1016/j.geoderma.2018.07.034

Bento, L.R., Melo, C.A., Ferreira, O.P., Moreira, A.B., Mounier, S., Piccolo, A., Spaccini, R., Bisinoti, M.C., 2020. Humic extracts of hydrochar and Amazonian Dark Earth: Molecular characteristics and effects on maize seed germination. Science of The

438 Total Environment 708, 1–11.
439 https://doi.org/10.1016/J.SCITOTENV.2019.135000

440 Bento, L.R., Spaccini, R., Cangemi, S., Mazzei, P., de Freitas, B.B., de Souza, A.E.O.,
441 Moreira, A.B., Ferreira, O.P., Piccolo, A., Bisinoti, M.C., 2021. Hydrochar
442 obtained with by-products from the sugarcane industry: Molecular features and
443 effects of extracts on maize seed germination. J Environ Manage 281.
444 https://doi.org/10.1016/j.jenvman.2020.111878

445 Canellas, L.P., Dantas, D.J., Aguiar, N.O., Peres, L.E.P., Zsögön, A., Olivares, F.L.,
446 Dobbss, L.B., Façanha, A.R., Nebbioso, A., Piccolo, A., 2011. Probing the
447 hormonal activity of fractionated molecular humic components in tomato auxin
448 mutants. Annals of Applied Biology 159, 202–211. https://doi.org/10.1111/j.1744-
449 7348.2011.00487.x

450 Canellas, L.P., Olivares, F.L., Okorokova-Façanha, A.L., Façanha, A.R., 2002. Humic
451 Acids Isolated from Earthworm Compost Enhance Root Elongation, Lateral Root
452 Emergence, and Plasma Membrane H+-ATPase Activity in Maize Roots. Plant
453 Physiol 130, 1951–1957. https://doi.org/10.1104/pp.007088

454 Castillo-Esparza, J.F., Bandala, V.M., Ramos, A., Desgarennes, D., Carrión, G., César,
455 E., Montoya, L., Ortiz-Castro, R., 2021. Pisolithus tinctorius extract affects the root
456 system architecture through compound production with auxin-like activity in
457 Arabidopsis thaliana. Rhizosphere 19, 100397.
458 https://doi.org/10.1016/j.rhisph.2021.100397

459 Chen, N., Cao, S., Zhang, Lin, Peng, X., Wang, X., Ai, Z., Zhang, Lizhi, 2021. Structural
460 dependent Cr(VI) adsorption and reduction of biochar: hydrochar versus pyrochar.

461 Science of The Total Environment 783, 147084.
462 https://doi.org/10.1016/j.scitotenv.2021.147084

463 Colla, G., Rouphael, Y., Canaguier, R., Svecova, E., Cardarelli, M., 2014. Biostimulant
464 action of a plant-derived protein hydrolysate produced through enzymatic
465 hydrolysis. Front Plant Sci 5, 1–6. https://doi.org/10.3389/fpls.2014.00448

466 Dell'Agnola, G., Nardi, S., 1987. Hormone-like effect and enhanced nitrate uptake
467 induced by depolycondensed humic fractions obtained from Allolobophora rosea
468 and A. caliginosa faeces. Biol Fertil Soils 4. https://doi.org/10.1007/BF00256983

469 D'Imporzano, G., Adani, F., 2007. The contribution of water soluble and water insoluble
470 organic fractions to oxygen uptake rate during high rate composting.
471 Biodegradation 18, 103–113. https://doi.org/10.1007/s10532-006-9045-y

472 Dobbss, L.B., Canellas, L.P., Olivares, F.L., Aguiar, N.O., Peres, L.E.P., Azevedo, M.,
473 Spaccini, R., Piccolo, A., Façanha, A.R., 2010. Bioactivity of chemically
474 transformed humic matter from vermicompost on plant root growth. J Agric Food
475 Chem 58, 3681–3688.
476 https://doi.org/10.1021/JF904385C/SUPPL_FILE/JF904385C_SI_002.PDF

477 Egamberdieva, D., Shurigin, V., Alaylar, B., Ma, H., Müller, M.E.H., Wirth, S., Reckling,
478 M., Bellingrath-Kimura, S.D., 2020. The Effect of Biochars and Endophytic
479 Bacteria on Growth and Root Rot Disease Incidence of Fusarium Infested Narrow-
480 Leafed Lupin (Lupinus angustifolius L.). Microorganisms 8, 1–16.
481 https://doi.org/10.3390/MICROORGANISMS8040496

482 Ertani, A., Cavani, L., Pizzeghello, D., Brandellero, E., Altissimo, A., Ciavatta, C., Nardi,
483 S., 2009. Biostimulant activity of two protein hydrolyzates in the growth and

484 nitrogen metabolism of maize seedlings. Journal of Plant Nutrition and Soil Science
485 172, 237–244. https://doi.org/10.1002/JPLN.200800174

486 Ertani, A., Pizzeghello, D., Baglieri, A., Cadili, V., Tambone, F., Gennari, M., Nardi, S.,
487 2013. Humic-like substances from agro-industrial residues affect growth and
488 nitrogen assimilation in maize (Zea mays L.) plantlets. J Geochem Explor 129, 103–
489 111. https://doi.org/10.1016/j.gexplo.2012.10.001

490 Farobie, O., Anis, L.A., Fatriasari, W., Karimah, A., Nurcahyani, P.R., Rahman, D.Y.,
491 Nafisyah, A.L., Amrullah, A., Aziz, M., 2022. Simultaneous production of
492 nutritional compounds and hydrochar from Chlorella pyrenoidosa via hydrothermal
493 process. Bioresour Technol Rep 20, 1–9.
494 https://doi.org/10.1016/j.biteb.2022.101245

495 Ferro, N., Gallegos, A., Bultinck, P., Jacobsen, H.J., Carbó-Dorca, R., Reinard, T., 2006.
496 Coulomb and overlap self-similarities: a comparative selectivity analysis of
497 structure-function relationships for auxin-like molecules. J Chem Inf Model 46,
498 1751–1762. https://doi.org/10.1021/CI050491C

499 Haris, M., Khan, M.W., Paz-Ferreiro, J., Mahmood, N., Eshtiaghi, N., 2022. Synthesis of
500 functional hydrochar from olive waste for simultaneous removal of azo and non-
501 azo dyes from water. Chemical Engineering Journal Advances 9, 100233.
502 https://doi.org/10.1016/j.ceja.2021.100233

503 Hou, P., Feng, Y., Wang, N., Petropoulos, E., Li, D., Yu, S., Xue, L., Yang, L., 2020.
504 Win-win: Application of sawdust-derived hydrochar in low fertility soil improves
505 rice yield and reduces greenhouse gas emissions from agricultural ecosystems.
506 Science of The Total Environment 748, 142457.
507 https://doi.org/10.1016/j.scitotenv.2020.142457

Ighalo, J.O., Rangabhashiyam, S., Dulta, K., Umeh, C.T., Iwuozor, K.O., Aniagor, C.O., Eshiemogie, S.O., Iwuchukwu, F.U., Igwegbe, C.A., 2022. Recent advances in hydrochar application for the adsorptive removal of wastewater pollutants. Chemical Engineering Research and Design 184, 419–456. https://doi.org/10.1016/j.cherd.2022.06.028

Kang, K., Nanda, S., Sun, G., Qiu, L., Gu, Y., Zhang, T., Zhu, M., Sun, R., 2019. Microwave-assisted hydrothermal carbonization of corn stalk for solid biofuel production: Optimization of process parameters and characterization of hydrochar. Energy 186, 115795. https://doi.org/10.1016/j.energy.2019.07.125

Kavindi, G.A.G., Lei, Z., Yuan, T., Shimizu, K., Zhang, Z., 2022. Use of hydrochar from hydrothermal co carbonization of rice straw and sewage sludge for Cr(VI) bioremediation in soil. Bioresour Technol Rep 18, 101052. https://doi.org/10.1016/j.biteb.2022.101052

Khosravi, A., Zheng, H., Liu, Q., Hashemi, M., Tang, Y., Xing, B., 2022. Production and characterization of hydrochars and their application in soil improvement and environmental remediation. Chemical Engineering Journal 430, 133142. https://doi.org/10.1016/j.cej.2021.133142

Lang, J., Matějová, L., Cuentas-Gallegos, A.K., Lobato-Peralta, D.R., Ainassaari, K., Gómez, M.M., Solís, J.L., Mondal, D., Keiski, R.L., Cruz, G.J.F., 2021. Evaluation and selection of biochars and hydrochars derived from agricultural wastes for the use as adsorbent and energy storage materials. J Environ Chem Eng 9, 105979. https://doi.org/10.1016/j.jece.2021.105979

Lang, Q., Liu, Z., Li, Y., Xu, J., Li, J., Liu, B., Sun, Q., 2022. Combustion characteristics, kinetic and thermodynamic analyses of hydrochars derived from hydrothermal

carbonization of cattle manure. J Environ Chem Eng 10, 106938. https://doi.org/10.1016/j.jece.2021.106938

Li, C., Cai, R., 2022. Preparation of solid organic fertilizer by co-hydrothermal carbonization of peanut residue and corn cob: A study on nutrient conversion. Science of The Total Environment 838, 1–12. https://doi.org/10.1016/j.scitotenv.2022.155867

Lin, H., Zhang, L., Zhang, S., Li, Q., Hu, X., 2022. Hydrothermal carbonization of cellulose in aqueous phase of bio-oil: The significant impacts on properties of hydrochar. Fuel 315, 123132. https://doi.org/10.1016/j.fuel.2022.123132

Liu, Q., Xu, R., Yan, C., Han, L., Lei, H., Ruan, R., Zhang, X., 2021. Fast hydrothermal co-liquefaction of corn stover and cow manure for biocrude and hydrochar production. Bioresour Technol 340, 1–11. https://doi.org/10.1016/j.biortech.2021.125630

Mariuzza, D., Lin, J.-C., Volpe, M., Fiori, L., Ceylan, S., Goldfarb, J.L., 2022. Impact of Co-Hydrothermal carbonization of animal and agricultural waste on hydrochars' soil amendment and solid fuel properties. Biomass Bioenergy 157, 106329. https://doi.org/10.1016/j.biombioe.2021.106329

Massaya, J., Mills-Lamptey, B., Chuck, C.J., 2022. Soil Amendments and Biostimulants from the Hydrothermal Processing of Spent Coffee Grounds. Waste Biomass Valorization 13, 2889–2904. https://doi.org/10.1007/S12649-022-01697-X/TABLES/5

Mohammadi, A., Anukam, A.I., Granström, K., Eskandari, S., Zywalewska, M., Sandberg, M., Aladejana, E.B., 2022. Effects of wood ash on physicochemical and morphological characteristics of sludge-derived hydrochar pellets relevant to soil

556 and energy applications. Biomass Bioenergy 163, 106531.
557 https://doi.org/10.1016/j.biombioe.2022.106531

558 Muscolo, A., 1999. Earthworm humic matter produces auxin-like effects on Daucus
559 carota cell growth and nitrate metabolism. Soil Biol Biochem 31, 1303–1311.
560 https://doi.org/10.1016/S0038-0717(99)00049-8

561 Nardi, S., Pizzeghello, D., Muscolo, A., Vianello, A., 2002. Physiological effects of
562 humic substances on higher plants. Soil Biol Biochem 34, 1527–1536.
563 https://doi.org/10.1016/S0038-0717(02)00174-8

564 NEN - Netherlands Normalisation Institute, 1994. NEN 5754. Determination of organic
565 matter content in soil as loss-on-ignition. Netherlands Normalisation Institute.

566 Pereira, R.C., Kaal, J., Camps Arbestain, M., Pardo Lorenzo, R., Aitkenhead, W., Hedley,
567 M., Macías, F., Hindmarsh, J., Maciá-Agulló, J.A., 2011. Contribution to
568 characterisation of biochar to estimate the labile fraction of carbon. Org Geochem
569 42, 1331–1342. https://doi.org/10.1016/J.ORGGEOCHEM.2011.09.002

570 Pizzeghello, D., Zanella, A., Carletti, P., Nardi, S., 2006. Chemical and biological
571 characterization of dissolved organic matter from silver fir and beech forest soils.
572 Chemosphere 65, 190–200. https://doi.org/10.1016/j.chemosphere.2006.03.001

573 Quaggiotti, S., 2004. Effect of low molecular size humic substances on nitrate uptake and
574 expression of genes involved in nitrate transport in maize (Zea mays L.). J Exp Bot
575 55, 803–813. https://doi.org/10.1093/jxb/erh085

576 Quevedo-Amador, R.A., Reynel-Avila, H.E., Mendoza-Castillo, D.I., Badawi, M.,
577 Bonilla-Petriciolet, A., 2022. Functionalized hydrochar-based catalysts for
578 biodiesel production via oil transesterification: Optimum preparation conditions

and performance assessment. Fuel 312, 122731. https://doi.org/10.1016/j.fuel.2021.122731

Santana, M.S., Alves, R.P., Santana, L.S., Gonçalves, M.A., Guerreiro, M.C., 2022. Structural, inorganic, and adsorptive properties of hydrochars obtained by hydrothermal carbonization of coffee waste. J Environ Manage 302, 1–11. https://doi.org/10.1016/j.jenvman.2021.114021

Scaglia, B., Pognani, M., Adani, F., 2015. Evaluation of hormone-like activity of the dissolved organic matter fraction (DOM) of compost and digestate. Science of the Total Environment 514, 314–321. https://doi.org/10.1016/j.scitotenv.2015.02.009

Sevilla, M., Fuertes, A.B., 2009. The production of carbon materials by hydrothermal carbonization of cellulose. Carbon N Y 47, 2281–2289.

Shuang, E., Jin, C., Liu, J., Yang, L., Yang, M., Xu, E., Wang, K., Sheng, K., Zhang, X., 2022. Engineering functional hydrochar based catalyst with corn stover and model components for efficient glucose isomerization. Energy 249, 123668. https://doi.org/10.1016/j.energy.2022.123668

Singh, H.P., Kaur, S., Batish, D.R., Kohli, R.K., 2014. Ferulic acid impairs rhizogenesis and root growth, and alters associated biochemical changes in mung bean (Vigna radiata) hypocotyls. J Plant Interact 9, 267–274. https://doi.org/10.1080/17429145.2013.820360

Spokas, K.A., 2010. Review of the stability of biochar in soils: Predictability of O:C molar ratios. Carbon Manag 1, 289–303. https://doi.org/10.4155/CMT.10.32/SUPPL_FILE/TCMT_A_10816161_SM0001.DOC

602 Sun, R., Zheng, H., Yin, S., Zhang, X., You, X., Wu, H., Suo, F., Han, K., Cheng, Y.,
603 Zhang, C., Li, Y., 2022. Comparative study of pyrochar and hydrochar on peanut
604 seedling growth in a coastal salt-affected soil of Yellow River Delta, China. Science
605 of The Total Environment 833, 155183.
606 https://doi.org/10.1016/j.scitotenv.2022.155183

607 Trevisan, S., Francioso, O., Quaggiotti, S., Nardi, S., 2010. Humic substances biological
608 activity at the plant-soil interface. Plant Signal Behav 5, 635–643.
609 https://doi.org/10.4161/psb.5.6.11211

610 USDA - United States Department of Agriculture, 2022. Production, Supply and
611 Distribution. https://apps.fas.usda.gov/psdonline/app/index.html#/app/advQuery
612 (acessed 15 Nov 2022).

613 Venkatesan, S., Baloch, H.A., Jamro, I.A., Rafique, N., 2022. Evaluation of the
614 production of hydrochar from spent coffee grounds under different operating
615 conditions. Journal of Water Process Engineering 49, 1–14.
616 https://doi.org/10.1016/j.jwpe.2022.103037

617 Wang, G., Zhang, J., Lee, J.Y., Mao, X., Ye, L., Xu, W., Ning, X., Zhang, N., Teng, H.,
618 Wang, C., 2020. Hydrothermal carbonization of maize straw for hydrochar
619 production and its injection for blast furnace. Appl Energy 266, 1–11.
620 https://doi.org/10.1016/J.APENERGY.2020.114818

621 Wang, M., Zhang, M., Chen, Xuhao, Chen, A., Xiao, R., Chen, Xinping, 2022.
622 Hydrothermal conversion of Chinese cabbage residue for sustainable agriculture:
623 Influence of process parameters on hydrochar and hydrolysate. Science of The
624 Total Environment 812, 152478. https://doi.org/10.1016/j.scitotenv.2021.152478

Wang, X., Sun, C., Gao, S., Wang, L., Shuokui, H., 2001. Validation of germination rate and root elongation as indicator to assess phytotoxicity with Cucumis sativus. Chemosphere 44, 1711–1721. https://doi.org/10.1016/S0045-6535(00)00520-8

Zandonadi, D.B., Santos, M.P., Busato, J.G., Eustáquio, L., Peres, P., Façanha, A.R., 2013. Plant physiology as affected by humified organic matter. Theor Exp Plant Physiol 25, 12–25.

Zhang, Y., Jiang, Q., Xie, W., Wang, Y., Kang, J., 2019. Effects of temperature, time and acidity of hydrothermal carbonization on the hydrochar properties and nitrogen recovery from corn stover. Biomass Bioenergy 122, 175–182. https://doi.org/10.1016/J.BIOMBIOE.2019.01.035

Zhang, Y., Qin, J., Yi, Y., 2021. Biochar and hydrochar derived from freshwater sludge: Characterization and possible applications. Science of the Total Environment 763, 144550. https://doi.org/10.1016/j.scitotenv.2020.144550

Declaration of interests

The authors declare that they have no known competing financial interests or personal relationships that could have appeared to influence the work reported in this paper.

In agreement,

Edson T.G. Lima

Erica D.S. Sales

Rogerio A. Saraiva

Ramom Rachide Nunes

CRediT – Contributor Roles Taxonomy

Edson T.G. Lima: data curation, formal analysis, methodology, writing – original draft.

Erica D.S. Sales: formal analysis.

Rogerio A. Saraiva: conceptualization, data curation, funding acquisition, methodology, supervision, writing – original draft.

Ramom Rachide Nunes: conceptualization, data curation, funding acquisition, methodology, supervision, project administration, writing – original draft, writing – review & editing.